

**INVESTIGATING THE POLLINATION PROCESS IN WIND-
POLLINATED PLANTS**

by

Claire Hass Smith

A thesis submitted to the Department of Biology

In conformity with the requirements for
the degree of Master of Science

Queen's University

Kingston, Ontario, Canada

September 2023

Copyright © Claire Hass Smith, 2023

Abstract

Despite its frequent evolution in the flowering plants, wind pollination has long been considered inefficient. Key traits of the wind pollination syndrome, high pollen production and low ovule number, have been thought to compensate for high pollen losses and a low probability of pollen capture. However, these traits may instead reflect selection by various processes to facilitate pollination, including the aerodynamics of wind pollination, selection related to sex system, correlated selection on pollen size and number, and the influence of local pollination conditions. Broadly, my thesis explores influences on wind pollination from both male and female perspectives, using field-collected data on pollen production, size and capture.

Pollen transfer efficiency, a measure of pollen transport loss, was similar between 19 wind-pollinated species and values previously reported for animal-pollinated species, suggesting wind pollination is not less efficient than animal pollination. Pollen size and number were negatively correlated in 6 of 23 species, indicating potential size-number tradeoffs. In all species, pollen size was significantly less variable than pollen number, suggesting pollen size is under stronger stabilizing selection. Pollen size but not production had a significant phylogenetic component, potentially because selection on the aerodynamics of pollen size is likely closely tied to plant architecture. Hermaphroditic species produced significantly more pollen per anther than monoecious, but not dioecious species, though this may be related to mating system.

Average stigmatic pollen loads exceeded ovule number for all 23 wind-pollinated species, suggesting that low ovule number resulting from a low probability of pollen receipt is unlikely. Instead, low ovule number may allow for increased pollen competition or represent a strategy to better sample the airstream by producing many inexpensive flowers. Stigma length and the timing of sampling within the flowering season strongly influenced pollen loads. Hermaphroditic

species captured more pollen than monoecious or dioecious species; however, much of this pollen may be self-pollen. Together, my results demonstrate the context-dependence of pollen receipt in wind pollination and challenge the assumption that wind pollination is inefficient, suggesting that high pollen production and low ovule number are unlikely to arise simply from a low probability of successful pollination.

Acknowledgements

I have so many people to thank for helping me complete this thesis. Thank you to the Friedman Lab. There's no one I'd rather not know what a fjord is with. Christina Steinecke and Aly Van Natto, for all the support and lab chats and introducing me to the NYT Crossword. Dr. Jannice Friedman, my gratitude for being such a supportive supervisor throughout all the twists and turns of this project. Isabeau Lewis, for help collecting samples in the field. Jeremiah Lee, for his keen attention to detail in counting pollen and his brilliance with ImageJ. Thank you to committee members, Drs. Chris Eckert, Troy Day and Bill Nelson for your helpful feedback. Thanks to Fruition Berry Farm for kindly letting me sample your weeds. And thank you to my friends and family, none of this would have been possible without you.

Table of Contents

Abstract.....	ii
Acknowledgements	iv
List of Figures	vii
List of Tables	ix
Chapter 1 Introduction.....	1
1.1 Introduction to wind pollination	1
1.2 Aerodynamics of wind pollination	3
1.2.1 Pollen release	3
1.2.2 Pollen transport	4
1.2.3 Pollen capture	5
1.3 Pollen size	6
1.4 Pollen production.....	7
1.5 Pollen size-number tradeoff	9
1.6 Individual-level effects on pollen capture	10
1.6.1 Effects of density on pollen capture.....	10
1.6.2 Effects of height on pollen capture	11
1.7 Predictions.....	12
Chapter 2 Methods	14
2.1 Study sites and species	14
2.2 Collecting and preparing samples.....	14
2.2.1 Quantifying pollen production and pollen size	14
2.2.2 Quantifying stigmatic pollen capture	16
2.3 Data analysis.....	16
2.3.1 Pollen production and size.....	16
2.3.1.1 Summary.....	16
2.3.1.2 Within-species pollen size-number tradeoff	17
2.3.1.3 Influence of sex system on pollen production.....	18
2.3.1.4 Effect of sex system on pollen size	19
2.3.2 Stigmatic pollen capture	20
2.3.2.1 Summary of stigmatic pollen capture	20
2.3.2.2 Individual-level effects on pollen capture.....	20
2.3.2.3 Effect of sex system on pollen capture	21

2.3 Pollination efficiency	22
Chapter 3 Results	23
3.1 Pollen production and pollen size	23
3.1.1 Summary	23
3.1.2 Within-species pollen size-number tradeoff	23
3.1.3 Influence of sex system on pollen production	24
3.1.4 Effect of sex system on pollen size	25
3.2 Stigmatic pollen capture.....	35
3.2.1 Summary	35
3.2.2 Individual-level effects on pollen capture	35
3.2.3 Effect of sex system on pollen capture.....	36
3.3 Pollination efficiency	43
Chapter 4 Discussion.....	47
4.1 Allocation to male reproduction	48
4.2 Evolution of ovule number.....	55
4.3 Influence of phylogeny	61
4.4 Summary	61
References.....	63
Appendix A Supplemental Tables.....	73
Appendix B Supplemental Figures.....	78

List of Figures

Figure 3-1. Relationship between pollen production per anther and pollen diameter for 23 wind-pollinated flowering plant species. Line of best fit shown in blue. Statistical details are shown in Table 3-2. 30

Figure 3-2. Mean pollen production per anther for dioecious (n=2), monoecious (n=9), and hermaphroditic (n=20) wind-pollinated flowering plant species. Left: Distribution of individual mean pollen production. Centre: Marginal mean (back-transformed) pollen production per sex system estimated from the linear mixed effects model. Error bars are 95% CIs. Letters represent the results of a pairwise Tukey’s HSD test at $\alpha=0.05$. Right: Bars represent species mean pollen production. 33

Figure 3-3. Mean pollen diameter for dioecious (n=2), monoecious (n=9), and hermaphroditic (n=20) wind-pollinated flowering plant species. Left: Distribution of individual mean pollen diameters. Centre: Marginal mean pollen size per sex system predicted from the mixed effects model. Error bars are 95% CIs. Letters represent the results of a pairwise Tukey’s HSD test at $\alpha=0.05$. Right: Bars represent species mean pollen diameters. 34

Figure 3-4. Distributions of pollen load for 23 wind-pollinated flowering plant species. Species’ sex systems are coded as follows: D = dioecious (green), M = monoecious (blue), H = hermaphroditic (orange). 39

Figure 3-5. Mean stigmatic pollen loads for dioecious (n=2), monoecious (n=9), and hermaphroditic (n=12) species. Left: Distribution of individual mean stigmatic pollen loads, with species pooled within sex systems. Centre: Marginal mean pollen loads per sex system predicted from the mixed effects model. Error bars are 95% CIs. Letters represent the results of a pairwise Tukey’s HSD test at $\alpha=0.05$. Right: Bars represent mean pollen loads per species. 42

Figure 3-6. The relationship between pollen production per flower and pollen capture per stigma for 19 wind-pollinated species. Error bars are standard deviations. Dotted lines represent 0.01%, 0.1%, 1%, and 10% pollen capture efficiency. 45

Figure 3-7. The relationship between pollen production per flower and pollen capture per stigma for 18 wind-pollinated species, *Thalictrum dioicum* excluded for better resolution between species. Error bars are standard deviations. Dotted lines represent 0.01%, 0.1%, 1%, and 10% pollen capture efficiency. 46

Figure B-1. Phylogeny of 32 wind-pollinated species used in the pollen production and size analysis, generated using the function “phylomaker” from the package “V.PhyloMaker2” (Jin & Qian 2022) using the seed plant phylogeny GBOTB.extended.TPL (Jin & Qian 2022) and the function’s default phylogenetic hypothesis scenario, Scenario 3 (Qian & Jin 2016). 78

Figure B-2. Phylogeny of 23 wind-pollinated species used in the pollen capture analysis, generated using the function “phylomaker” from the package “V.PhyloMaker2” (Jin & Qian 2022) using the seed plant phylogeny GBOTB.extended.TPL (Jin & Qian 2022) and the function’s default phylogenetic hypothesis scenario, Scenario 3 (Qian & Jin 2016). 79

Figure B-3. Relationship between stigmatic pollen load (pollen/ovule) and sampling date. Line of best fit shown in blue. 80

Figure B-4. Relationship between stigmatic pollen load (pollen/ovule) and plant height (cm). Line of best fit shown in blue. 81

Figure B-5. Relationship between stigmatic pollen load (pollen/ovule) and density, shown as the inverse of the average distance to a plant’s 5 nearest pollen-producing neighbours (cm^{-1}). Line of best fit shown in blue. 82

Figure B-6. Relationship between stigmatic pollen load (pollen/ovule) and stigma length (cm) for 13 wind-pollinated plants. Line of best fit shown in blue. 83

List of Tables

Table 3-1. Summary of pollen size (pollen diameter, μm) and number (pollen per anther) for 31 wind-pollinated flowering plant species. For the column “Sex system”, D = dioecious, M = monoecious, H = hermaphroditic. The number of individuals measured per species is listed as N.....	27
Table 3-2. Summary of linear regression models predicting pollen production by size as $\log(\text{pollen per anther}) \sim \log(\text{pollen diameter})$ for each of 23 wind-pollinated flowering plant species. The regression slope represents the exponent a in the relationship $\log(n) = \log(cs^a)$, where n is the number of pollen grains per anther, s is pollen grain diameter, and c is a constant. For the column “Sex system”, D = dioecious, M = monoecious, H = hermaphroditic. Significant p -values (<0.05) for the slope of pollen diameter are bolded. See Figure 3-1 for depictions of the data and the regression line.	31
Table 3-3. Stigmatic pollen loads for 23 wind-pollinated species. Species’ sex systems are coded as follows: D = dioecious, M = monoecious, H = hermaphroditic. N represents the number of individuals measured per species.	38
Table 3-4. Summary of results from mixed models predicting the relationship between stigmatic pollen receipt and individual-level factors for 13 wind-pollinated species. Table shows coefficients (β), standard errors, t -values, and corresponding p -values for linear models generated using model selection with dredge, from the full model $\log(\text{pollen}) \sim \text{date} + \text{height} + 1/\text{density} + \text{stigma length} + (1 \text{plant})$. When multiple models had indistinguishable explanatory power ($\Delta\text{AICc} < 2$), the fullest model was considered as the top model (bolded, when applicable).....	40
Table 3-5. Pollination efficiency for 19 wind-pollinated flowering plant species. Pollination efficiency is calculated as mean pollen production per flower/mean stigmatic pollen load $\times 100\%$	44
Table A-1. Sampling details and list of all species where pollen production and size were quantified. N is the number of individuals measured per species.	73
Table A-2. Sampling details and list of all species where stigmatic pollen receipt was quantified. N is the number of individuals measured per species.	75
Table A-3. Sampling details and list of all species used to analyze the effects of individual-level factors on stigmatic pollen receipt. Species are ordered first by sex system, then alphabetically. N is the number of individuals measured per species.	76
Table A-4. Summary of individual-level factors potentially affecting pollen capture for 13 wind-pollinated species. Plant height is a plant’s maximum height in cm, stigma length is the maximum length of a plant’s stigma in cm, and density is measured as the average distance from a plant to its five-nearest pollen-producing neighbours, in cm.	77

Chapter 1

Introduction

1.1 Introduction to wind pollination

The flowering plants have evolved a diversity of pollination strategies, ranging from complex coevolutionary relationships with specialized animal pollinators to strategies that are completely abiotic, using wind or water currents to transport pollen. Animal pollination is the ancestral condition in the flowering plants (Hu et al. 2008) and remains the primary pollination mode of approximately 87.5% of extant flowering plant species today (Ollerton et al. 2011). Of the species that instead rely on abiotic pollination, wind pollination is the most common strategy, making up around 98% of known cases (Faegri and Van der Pijl 1979) and occurring in ~18% of flowering plant families (Ackerman 2000). Transitions from animal pollination to wind pollination in the flowering plants have occurred at least 65 times, across diverse lineages (Linder 1998). While many wind-pollinated species belong to primarily wind-pollinated families, like the grasses (Poaceae), sedges (Cyperaceae), and rushes (Juncaceae), others have evolved as outliers within primarily animal-pollinated families, including the Amaranthaceae (e.g., *Amaranthus*), Ranunculaceae (e.g., *Thalictrum*), and the Asteraceae (e.g., *Ambrosia*).

Despite how frequently wind pollination evolves, it has long been considered to be an undirected, wasteful process where “pollen grains are scattered by chance and the percentage of ... effective pollen grains [reaching the stigma] is almost infinitely small” (Faegri and Van der Pijl 1979). Because of this, many common features of wind-pollinated plants have been understood as mechanisms to compensate for this inefficiency, like the tendency for wind-

pollinated plants to produce large volumes of pollen but package only one (or few) ovules per carpel (Faegri and Van der Pijl 1979, Ackerman 2000, Friedman and Barrett 2009b).

Correspondingly, wind-pollinated plants tend to have relatively high pollen:ovule ratios, a metric often used to compare pollen production between species. High pollen:ovule ratios have been thought to signify low pollination efficiency since Cruden (2000) popularized this idea.

However, many wind-pollinated plants receive more than enough pollen to set seed. For example, in *Staberoha banksii*, mean pollen loads ranged from 4.4 to 28 grains per stigma and 5.19 pollen tubes per uni-ovulate pistil (Honig et al. 1992). Observations like this suggest that despite their high pollen:ovule ratios, wind-pollinated species may not be as inefficient as previously thought.

In addition to producing large volumes of pollen and few ovules, many wind-pollinated species share a similar set of traits thought to facilitate pollen transfer by the wind. Most wind-pollinated species make small, inconspicuous flowers that are green or white; have small or no petals; have exposed anthers and stigmas; produce non-sticky, unornamented pollen grains; and frequently have unisexual flowers (Faegri and Van der Pijl 1979, Friedman and Barrett 2008). Transitions from animal to wind pollination are associated with reductions in floral display, reductions in floral scent and colour, and the absence of nectar rewards, suggesting these traits are functional in animal- but not wind-pollinated plants (Welsford et al. 2016). Making attractive structures like large, colourful petals is costly and could interfere with pollen export or receipt by the wind. Rather than being adapted to attract animal pollinators, wind-pollinated flowers are instead adapted for the aerodynamics of wind pollination.

For successful wind pollination to occur, pollen grains must be released into the airstream, dispersed to a neighbouring plant, and captured by a recipient stigma (Whitehead

1969). The processes of pollen release, transport, and capture each have their own set of aerodynamic challenges and require corresponding biomechanical adaptations (Niklas 1992). In the next section, I will describe these three processes, including the aerodynamic challenges they pose and how wind-pollinated plants have adapted in response.

1.2 Aerodynamics of wind pollination

1.2.1 Pollen release

For pollen to be picked up by the wind, it must be acted on with enough force to overcome the molecular adhesion holding pollen to anthers. Wind gusts with enough force may apply sufficient lift or drag that grains separate from the anther surface and are released into the airstream. However, all plant surfaces interacting with the wind, including leaves, stems, stigmas, and anthers, are surrounded by a boundary layer of still air, proportional to the surface's size. This complicates pollen removal, as windspeeds within the boundary layer decrease along a velocity gradient, slowing to nearly zero next to an object's surface (Niklas 1992). Because of this, windspeeds close to pollen grains can be greatly reduced (Urzay et al. 2009). As a result, many plants have evolved adaptations to minimize boundary layer effects on pollen removal. For example, many grass anthers have long filaments that extend perpendicularly away from their inflorescences and many wind-pollinated trees package their anthers on catkins that dangle into the airstream below their branches (Harder and Prusinkiewicz 2013). By positioning anthers outside the plant's innermost boundary layers, these adaptations may facilitate pollen removal by exposing anthers to higher windspeeds.

An alternate strategy to directly blowing pollen off anthers, wind gusts may facilitate pollen release by causing stamens to vibrate or shake. When wind gusts set stamens in motion, pollen grains attached to anthers will resist sudden changes in motion and the inertia can send

them into the airstream like dust off a beaten carpet (Niklas 1992, Urzay et al. 2009). Further, when wind gusts vibrate stamens at their natural frequency, they may experience resonance, a phenomenon where they oscillate with greater amplitude than if the same force were applied at a different frequency, allowing stamens to eject pollen from their anthers with greater force than aerodynamic forces alone (Timerman et al. 2014). Stamen resonance is a key process for pollen release in several wind-pollinated species, including *Plantago lanceolata* (Timerman et al. 2014) and many species of the genus *Thalictrum* (Timerman and Barrett 2019). Additionally, vortex shedding, the phenomenon that induces stamen resonance, only occurs when windspeeds are above a certain threshold (Niklas 1992). Since greater windspeeds allow pollen to travel further from its source, this means that pollen release facilitated through stamen resonance may be particularly useful in ensuring long-distance dispersal.

1.2.2 Pollen transport

Once it is picked up by the wind, a pollen grain drifting through the airstream experiences two key forces: gravity, pulling it downward and causing it to eventually settle out of the airstream, and lateral displacement by the wind, transporting it away from its source (Niklas 1985). In general, the longer it takes a grain to settle out of the airstream, the farther it can travel. The rate at which pollen settles can be estimated using Stokes' Law, which describes the maximum settling velocity of a sphere falling in a fluid: $V_s = \frac{2r^2g(\rho-\rho_0)}{9\mu}$, where r is the radius of a sphere, ρ and ρ_0 are the density of the object (pollen grain) and the air, respectively, and μ is the dynamic viscosity of air (Niklas 1992). Hence, smaller and lighter pollen grains will have lower settling velocities than larger and heavier grains, allowing them to travel further before settling out of the airstream.

How quickly pollen settles out of the airstream will also depend on the height from which pollen is released. In general, pollen released from greater heights should remain in the airstream longer and disperse further (Burd and Allen 1988, Okubo and Levin 1989). The higher the release point, the further pollen has to travel before settling out, and the further it can be blown horizontally by the wind (Niklas 1985). Additionally, because of the earth's boundary layer, windspeeds increase logarithmically from the ground up (Niklas 1992), so that pollen released from greater heights should be subject to stronger winds that can aid in dispersal. Because of this, taller plants may have an advantage in dispersing pollen.

1.2.3 Pollen capture

After pollen is picked up by the wind and transported through the airstream, it must cross an additional boundary layer to successfully land on a stigma. The chance that a pollen grain will be successfully captured by a stigma depends on stigma size, pollen size, and windspeed (Paw U and Hotton 1989). Larger stigmas will have more surface area to sample the airstream but will also have larger boundary layers that will tend to deflect pollen (Niklas 1992). This leads to an empirical relation between pollen and receptor size in wind-pollinated species. For example, grass species with larger inflorescences tend to produce larger (heavier) pollen grains (Friedman and Harder 2005). The larger grains are more likely to achieve the momentum necessary to break through these inflorescences' thick boundary layers.

Pollen capture in wind-pollinated species can also be highly specific. Wind-tunnel analyses demonstrate that wind-pollinated species create unique airflow patterns around their flowers so that they preferentially capture conspecific pollen (Niklas 1982, 1984, Niklas and Paw U 1982), even among sympatric species of the same genus (e.g. *Ephedra trifurca* and *E.*

nevadensis) (Niklas and Buchmann 1987). In this way, inflorescences can act like centrifuges that sort through airborne pollen according to their size and density.

1.3 Pollen size

The processes of pollen release, transport, and capture described in Section 1.2 impose conflicting selective pressures on pollen size. While smaller, lighter pollen is more easily removed from anthers and transported further due to its low settling velocity; larger, heavier pollen has greater momentum, making it more likely to successfully impact a stigma (Whitehead 1969). Balancing selection from these conflicting pressures may explain why pollen size varies relatively little among wind-pollinated species (17-58 μm) (Whitehead 1969) compared to animal-pollinated species (5-250 μm) (Wodehouse 1935, Muller 1979).

In addition to selection imposed during pollen transport by the wind, selection on pollen size may also occur after pollen is deposited on stigmas. Post-pollination processes like pollen germination, pollen tube growth, and ovule fertilization are key in determining pollen size in animal-pollinated plants (Harder 1998). Pollen size is associated with competitive ability during pollen tube growth down the style to the ovary, with larger pollen having more resources available for faster germination and growth (Baker and Baker 1979). Larger pollen size has been demonstrated to correlate with competitive ability in *Ipomoea purpurea*, where larger grains outcompeted smaller grains during pollen competition in plants with genetically-determined differences in pollen size (McCallum and Chang 2016). The effects of pollen competition may be especially strong in wind-pollinated plants because most have just a single ovule per flower and pollen release tends to be highly synchronous (Dowding 1987), which could allow multiple grains to arrive and germinate on a stigma at once. Therefore, the same processes involved in post-pollination selection on pollen grain size in animal-pollinated plants are likely also present

if not stronger in wind-pollinated species, potentially favouring larger grains when competition between grains is high.

1.4 Pollen production

In contrast with their low ovule production, wind-pollinated species tend to produce large quantities of pollen (Proctor and Yeo 1973, Ackerman 2000, Michalski and Durka 2009, 2010). This high pollen production, especially in contrast to their low ovule number, is typically thought to reflect inefficient pollen transfer (Cruden 1977, 2000). If female fitness is pollen-limited, then plants may produce large amounts of pollen to compensate for pollen losses during transport and ensure successful pollination (Harder and Johnson 2023). For example, in a study of 51 animal-pollinated species, pollen production declined with increasing pollen transfer efficiency (percentage of pollen removed from flowers that reached stigmas) (Harder and Johnson 2023). However, while pollen limitation appears widespread in animal-pollinated plants (Knight et al. 2005), it may be less common in wind-pollinated plants (Friedman and Barrett 2009b), suggesting that other factors may play important roles in the high pollen production of wind-pollinated plants.

High pollen production in wind-pollinated species compared to animal-pollinated species may be associated with differences in the shape of the male fitness gain curve, which describes the relationship between male fitness and investment in male function. In animal-pollinated species, male gain curves likely saturate because the benefits from investing more into male function may eventually be limited by pollinator behaviour, like pollen grooming by bees (Charnov 1979, Harder and Thomson 1989, Klinkhamer et al. 1997). In contrast, the male gain curve in wind-pollinated plants should be more linear because the wind is not limited by how much pollen it can carry and pollen loss is independent of pollen production (Charlesworth and

Charlesworth 1981, Charnov 1982, Klinkhamer and de Jong 1997). While characterizing male gain curves is technically challenging, evidence for a linear male gain curve has been observed in white spruce (Schoen and Stewart 1986) and ragweed (Aljiboury and Friedman 2022).

Correspondingly, wind-pollinated plants may produce more pollen relative to animal-pollinated plants because they receive greater fitness benefits from investing more into male function.

Pollen production in wind-pollinated species is also likely influenced by sex system. Dioecious species may produce more pollen than cosexual species. For example, in androdioecious *Mercurialis annua*, dioecious individuals produce ~10 times the pollen of monoecious individuals (Hesse and Pannell 2011b). There may be several reasons for this higher investment in pollen production in dioecious species. In species with separate sexes, the average distance between potential mates will be greater than for cosexual plants, assuming equal population densities (Cruden 2000). Since the dispersal of wind-borne pollen tends to have a distribution that declines rapidly with distance, dioecious species may experience greater pollen loss during transport than hermaphroditic or monoecious species and may produce more pollen to account for these losses. Additionally, species with unisexual flowers may be able to produce more pollen than those with cosexual flowers because they do not pay the fixed resource costs of building both male and female reproductive structures within the same flower. Instead, more resources can be invested in gamete production. In a comparative study of 291 herbaceous wind-pollinated species, pollen production per flower was significantly high in dioecious and monoecious species than in hermaphroditic species (Michalski and Durka 2010). However, the patterns of pollen production reported in that study may be better explained by mating system than sexual system, explained below.

A species' ability to self-fertilize is a key determinant of pollen production. The above pattern of higher pollen production in dioecious and monoecious species and lower pollen production in hermaphroditic species disappeared when woody perennials were added to the analysis, which had higher pollen production than herbaceous species independent of sex system (Michalski and Durka 2010). This may be because long-lived woody species are often outcrossing, because their long lifespans lead to strong selection against self-fertilization (Scofield and Schultz 2005). Pollen production tends to be higher in outcrossing species, which may explain the relatively higher pollen production in woody perennials and dioecious and monoecious herbaceous species, since dioecious species cannot self-fertilize and monoecious species are often self-incompatible (Proctor et al. 1996). An association between self-fertilization and lower pollen production has also been observed in wind-pollinated members of the genus *Plantago*, where outcrossing species produced significantly more pollen than those with closed, self-pollinating flowers (Primack 1978).

1.5 Pollen size-number tradeoff

Pollen production and pollen size may experience correlated selection. If plants have a limited resource budget for male function, a trade-off between pollen size and number may arise if resources are split between making either many small grains or fewer large grains. Negative phenotypic associations between pollen size and number occur across related species in the papilionaceous legumes (Vonhof and Harder 1995), within the genus *Pedicularis* (Yang and Guo 2004) as well as within species (Vonhof and Harder 1995, Parachnowitsch and Elle 2004, Milatović et al. 2020). Negative genetic correlations between pollen size and number have been observed (Mazer and Hultgård 1993, Stanton and Young 1994, Sarkissian and Harder 2001). Artificial selection experiments on pollen size in *Brassica rapa* found that selection within

genetic lines for small-diameter pollen also resulted in the production of significantly more pollen, compared to lines with selection for large pollen. However, total pollen volume did not differ between selection lines, suggesting that a size-number tradeoff arose from flowers having fixed resource budgets for pollen production (Sarkissian and Harder 2001). A negative genetic correlation between pollen size and number may constrain the evolution of both traits. For example, if increasing pollen size tends to decrease pollen numbers, then fitness benefits from greater post-pollination competitive ability by larger pollen may be offset by decreased fitness from lower pollen numbers. Since pollen size is highly constrained by the aerodynamics of pollen transport in wind-pollinated species, if a pollen size-number tradeoff exists, a species' optimal pollen size-number values may reflect its optimal pollen size for successful transport, rather than its optimal pollen number for dispersal.

1.6 Individual-level effects on pollen capture

1.6.1 Effects of density on pollen capture

Pollen capture in a population of wind-pollinated plants may be closely tied to the population's density. Wind-borne pollen dispersal tends to be highly leptokurtic, with most pollen deposited close to its source and decreasing quickly beyond that (Bateman 1947, Gleaves 1973, Levin and Kerster 1974, Tonsor 1985, Rognli et al. 2000). Because of this, wind pollination can be highly local. For example, in the broadleaf cattail *Typha latifolia*, spatial simulations of pollen dispersal estimated that nearly 99% of pollen disperses less than 2m from its source. As a result of the local nature of wind pollination, plants with fewer pollen-producing neighbours tend to receive lower pollen loads and have lower seed set. This has been observed in several wind-pollinated species. Isolated females in low-density populations were pollen limited

in two dioecious *Thalictrum* species (Steven and Waller 2007). In *Rumex nivalis*, also dioecious, pollen loads and seed set were greater in females in closer proximity to males (Stehlik et al. 2008). As such, the local density of pollen-producing neighbours around a plant appears to strongly influence pollen capture.

The effects of density may also vary depending on a species' sex system. Hermaphroditic or monoecious species capable of self-fertilization may seldom experience pollen limitation due to low density by ensuring pollen receipt through self-pollination. For example, in *Mercurialis annua*, a self-compatible (wind-pollinated) herb with both monoecious and dioecious populations, monoecious plants had increased selfing rates at decreased population densities (Eppley and Pannell 2007). Correspondingly, pollen limitation has been observed in low-density patches of dioecious, but not monoecious, *M. annua* (Hesse and Pannell 2011a). As a result, pollen capture in dioecious species may be more sensitive to local density than monoecious or hermaphroditic species.

1.6.2 Effects of height on pollen capture

Plant height is uniquely important in wind-pollinated plants because of the aerodynamics of wind pollination. As described in Section 1.2, taller plants can disperse their pollen over a wider area, increasing the chances of their pollen colliding with a receptive stigma (Burd and Allen 1988). In contrast, shorter plants may be better suited to capture pollen because they are more likely to fall within the pollen shadow of other plants. These opposing benefits of height to pollen dispersal and pollen capture are apparent in wind-pollinated species that allocate differently to male or female function, depending on their height. Size-dependent sex allocation has been well-described in the monoecious wind-pollinated herb *Ambrosia artemisiifolia* (McKone and Tonkyn 1986, Ackerly and Jasieński 1990, Traveset 1992, Lundholm and Aarssen

1994). When plant height is controlled by shading treatments, shorter plants tend to produce more female flowers (Paquin and Aarssen 2004, Friedman and Barrett 2009b) while taller, unshaded plants tend to produce more male flowers (Friedman and Barrett 2009b). If plants can sense their relative height in a population based on how much shade they receive, they can optimize their investment in either pollen production or pollen capture.

1.7 Predictions

In this thesis, I aim to understand the strategies wind-pollinated plants use to facilitate successful pollination from both male and female fitness perspectives. Using field-collected data on pollen size, production, and stigmatic pollen capture, I explore how these traits vary within and between wind-pollinated species and how they relate to each other.

I first focus on male function and investigate how pollen size and pollen number vary both within and across 31 wind-pollinated species (1.1); I test for a pollen size-number tradeoff within species (1.2); and I explore how sex system influences pollen production (1.3) and pollen size (1.4) across species. Specifically, I test whether dioecious species make more and smaller pollen, to compensate for separation of the sexes. I then turn to female function and explore how patterns of pollen capture per stigma vary across 23 wind-pollinated species (2.1); whether pollen capture is influenced by factors such as plant height, stigma length, sampling date, or local density (2.2); and how sex system influences pollen capture, specifically testing whether pollen capture is highest in hermaphroditic species and lowest in dioecious species (2.3). Lastly, I calculate pollen transfer efficiency (PTE) for 19 wind-pollinated species to explore how PTE in wind-pollinated species compares to values previously reported for animal-pollinated species (Harder 2000) (3). Broadly, I aim to describe patterns of pollen receipt and production in wind-

pollinated plants and explore how wind-pollinated plants from diverse families and sex systems facilitate successful pollination despite the inherent stochasticity in wind pollination.

Chapter 2

Methods

2.1 Study sites and species

I quantified pollen production, pollen size, and stigmatic pollen capture in herbaceous wind-pollinated flowering plant species sampled near Kingston, ON in 2021, Kananaskis, AB in 2001, and the Koffler Scientific Reserve near Newmarket, ON in 2004. All species were sampled during their peak flowering in the spring or summer months. The species sampled belonged to diverse families, including the Amaranthaceae, Asteraceae, Cyperaceae, Plantaginaceae, Poaceae, Polygonaceae, and Ranunculaceae. Across all sampling sites, pollen size and production were measured for 31 species, including 2 dioecious species, 9 monoecious species, and 20 hermaphroditic species (Table A-1). Pollen capture was measured in a total of 23 species across all field sites, including 2 dioecious, 9 monoecious, and 12 hermaphroditic species (Table A-2).

2.2 Collecting and preparing samples

2.2.1 Quantifying pollen production and pollen size

In field sites around Kingston, Ontario, I collected at least 3 undehisced anthers from 7 wind-pollinated species, from at least 5 individuals per species. I collected anthers into microcentrifuge tubes filled with 0.5mL 70% ethanol and stored them at 4°C. To quantify pollen production and size, I released pollen from anthers by gently crushing them with a stir stick, and sonicated the tubes in an ultrasonic bath for 30 min to dislodge any remaining pollen from anther walls. I pipetted 3 subsamples of suspended pollen from each tube onto a glass slide, stained the

pollen with 1% fuschin dye, and counted the number of grains per subsample using a Leica DMi8 microscope at 5x magnification. I scaled this subsample count by the total volume of liquid in the sample to calculate the total number of pollen grains per anther. Pollen counts per subsample were done either by eye or by taking images of subsamples at 5x magnification and using an ImageJ-based (Schneider et al. 2012) pollen-counting program to count the number of grains present. For *Amaranthus retroflexus*, *Ambrosia artemisiifolia*, *Chenopodium album*, *Plantago lanceolata*, and *Setaria viridis*, I counted pollen grains manually. For *Rumex acetosella* and *Thalictrum dioicum*, I counted grains using the ImageJ automated particle counting program.

The same samples were also used to quantify pollen size. I pipetted at least 3 subsamples per sample onto a slide, which were then photographed using a camera mounted on a dissection microscope. For better imaging, each subsample was mixed with a drop of 50% glycerol solution to promote suspension and a drop of soap solution to prevent clumping. All pollen size measurements were done using a custom ImageJ script to measure particle area, except for *Setaria viridis*, where there was too much debris in sample solutions for the program to function properly and pollen size was instead measured as pollen diameter using the measurement tool within Leica LASX microscope software.

For species sampled by Jannice Friedman in Kananaskis, AB (2001-2002) and Koffler Scientific Reserve, ON (2004), anthers were collected in the field in the same way as above for 30 wind-pollinated flowering plant species, from at least 3 individuals per species. Pollen production and size were quantified using an Elzone 5380 particle counter (Micromeritics Inc., Atlanta, GA).

2.2.2 Quantifying stigmatic pollen capture

During the 2021 field season in Kingston, ON, I collected stigma-bearing flowers from the field into microcentrifuge tubes filled with 70% ethanol and stored at 4°C. I collected at least 1-3 stigma-bearing flowers per individual, with a minimum of 15 individuals per species. For each individual, I recorded plant height and the distance to a plant's five nearest pollen-bearing neighbours. To quantify pollen capture, stigmas were carefully removed from flowers, stained with 1% fuschin dye, and gently squashed under a glass cover slip. I then recorded the total number of conspecific pollen grains on each stigma, viewed under 5x-20x magnification using a Leica DMI8 microscope. In *Thalictrum dioicum*, stigmas required an overnight soak in 1M NaOH to clarify their dark stigmatic tissue and increase the visibility of pollen grains under the microscope.

For the species collected by Jannice Friedman in Kananaskis, AB (2001-2002) and Koffler Scientific Reserve, ON (2004), flowers were similarly sampled from the field and their pollen loads were similarly counted. In addition, stigma length was measured under the microscope for these species. All species have a single ovule per carpel, except *Plantago lanceolata*, which has two (Henderson 1926).

2.3 Data analysis

All analyses were performed in R 4.3.1 (R Core Team 2023). Data and analysis scripts can be found on GitHub, at <https://github.com/claireasmith/masters-thesis.git>. All visualizations were created using ggplot2 (Wickham 2016).

2.3.1 Pollen production and size

2.3.1.1 Summary

I quantified patterns of pollen production and size by calculating summary statistics (mean, sd, min, max, CV) for each species. I tested whether pollen size tended to be more variable than pollen production across species using a paired t-test comparing each species' CV in pollen size against its CV in pollen production. For all measures of pollen size variation I used pollen diameter as a measure of pollen size; for the pollen size-number tradeoff I used volume to better account for allometric relationships.

2.3.1.2 Within-species pollen size-number tradeoff

I tested for a within-species tradeoff in pollen production and size in all species with at least 10 individuals, a total of 23 species. Assuming each flower has a fixed budget for pollen production, e , I modeled the relationship between pollen size and number as $n \propto es^a$, where n is the number of pollen grains per anther, s is pollen grain volume, and a is a constant determining the shape of the relationship between pollen number and volume. If we let c be some constant that incorporates e and converts units of pollen volume to pollen grains per anther, then this relationship can be written as $n = cs^a$. If pollen size and number trade off, then a should be negative.

For each species, I tested for a pollen size-number tradeoff by log-transforming both sides of this equation and estimating the parameter a and the intercept $\log(c)$, as $\log(n) = \log(cs^a) = \log(c) + a \log(s)$. Specifically, I built a linear model of the form $\log(\text{pollen production}) \sim \log(\text{pollen volume})$, where pollen production is the average number of pollen grains produced per anther and pollen size is pollen volume in μm , and tested whether the slope of the pollen size term was significantly different from zero. Pollen volume was estimated from pollen diameter as the volume of a sphere.

I chose to examine pollen size and production at the per-anther level for several reasons. First, flowers likely act as individual units that draw resources locally and cannot share resources among one another (Casper and Niesenbaum 1993). Second, inflorescence architecture, including the number of anthers per flower, flowers per inflorescence, and inflorescences per plant, varies widely across wind-pollinated flowering plants. For example, *Thalictrum dioicum* has 16-28 anthers per flower (pers. obs), while most grasses have just 3 anthers per flower. As such, anthers were chosen as the most comparable unit across species.

2.3.1.3 Influence of sex system on pollen production

Next, I tested whether a species' sex system influenced its pollen production. To account for potential nonindependence between species due to their phylogenetic history, I used phylogenetic least squares (PGLS) regression. Specifically, I tested whether pollen production tended to be higher in dioecious species than monoecious or hermaphroditic species using the phylogenetic least squares model $\log(\text{pollen production}) \sim \text{pollen size} + \text{sex system}$. Log(pollen production) is the log-transformed pollen production per anther, averaged for a species, pollen size is a species' average pollen diameter in μm , and sex system is a categorical predictor for a species' sex system (dioecious, monoecious, or hermaphroditic). I included pollen size in the model to account for a potential across-species tradeoff in pollen size and number.

I used all species with at least 3 individuals for this analysis. This included a total of 31 species, with 2 dioecious species, 9 monoecious species, and 20 hermaphroditic species. Before fitting the PGLS models, I inspected the distributions of predictors and the response variable for outliers or strong asymmetry that might give large values undue influence. Correspondingly, I log-transformed pollen production to make its distribution more symmetric. I also checked for

potential collinearity between predictors using the function “vif” from the package “car” (Fox and Weisberg 2019).

I fit the PGLS model with the function “pgls” from the package “caper” (Orme et al. 2018), using maximum likelihood to estimate the parameter branch length scaling parameter λ and using a phylogenetic variance-covariance matrix of branch lengths based on a phylogenetic tree of the 31 species used in this analysis (Figure B-1). This phylogeny was built using the function “phylomaker” from the package “V.PhyloMaker2”, using the seed plant phylogeny GBOTB.extended.TPL and the function’s default phylogenetic hypothesis scenario, Scenario 3 (Qian and Jin 2016, Jin and Qian 2022).

Since the PGLS model necessarily uses species-level data, it obscures any within-species variation in pollen production. To account for this, I also ran a linear mixed effects model on individual-level data. I restricted this analysis to species with at least 10 individuals, which resulted in a dataset of 23 species, including 2 dioecious, 8 monoecious, and 13 hermaphroditic species. To account for different species potentially having different pollen size-number relationships, I included a random-slope term for pollen size, $\log(\text{pollen production}) \sim \log(\text{pollen volume}) + \text{sex system} + (\log(\text{pollen volume})/\text{species})$. I tested whether this random-slope term improved on a model with a random-intercept term for species, of the form $\log(\text{pollen production}) \sim \log(\text{pollen volume}) + \text{sex system} + (1/\text{species})$, using the *anova()* function. All linear models were built using “lmer” from the package “lme4” (Bates et al. 2015). I estimated marginal means for pollen production for each sex system from the mixed effects model using the function “emmeans” from the package “emmeans” (Lenth 2023). I used a Tukey’s HSD post-hoc test to test for pairwise differences in pollen production between the different sex systems.

2.3.1.4 Effect of sex system on pollen size

I tested whether sex system influenced a species' pollen size using a similar framework to that described above. To test whether dioecious species tend to make smaller pollen than monoecious or hermaphroditic species, I fit a PGLS model of the form $\log(\text{pollen size}) \sim \text{sex system}$ using “pgls” from “caper” (Orme et al. 2018), using maximum-likelihood to estimate λ . As above, the dataset included a total of 31 species with at least 3 individuals per species, with 2 dioecious species, 9 monoecious species, and 20 hermaphroditic species. Before fitting the PGLS models, I inspected the distributions of predictors and the response variable and checked for potential collinearity between predictors.

I also ran a linear mixed effects model with a random-intercept term for species, $\text{pollen size} \sim \text{sex system} + (1/\text{species})$ using “lmer” (Bates et al. 2015), calculated estimated marginal means for pollen size for each sex system using “emmeans” (Lenth 2023), and used a Tukey's HSD post-hoc test to test for pairwise differences in pollen size between the different sex systems.

2.3.2 Stigmatic pollen capture

2.3.2.1 Summary of stigmatic pollen capture

I quantified overall patterns of pollen capture by calculating summary statistics (mean, sd, min, max, CV) for each species. For a more complete visualization of pollen capture patterns, I plotted distributions of pollen capture per uni-ovulate flower for all species using the “ggridges” package (Wilke 2022).

2.3.2.2 Individual-level effects on pollen capture

For a subset of 13 species (Table A-3), I tested whether the amount of per-ovule pollen a flower receives could be predicted by sampling date, plant height, the local density of pollen

producers, or stigma length. For each species, I fit a linear mixed effects model of the form $\log(\text{pollen receipt}) \sim \text{date} + \text{height} + 1/\text{density} + \text{stigma length} + (1|\text{plant})$ using “lmer” from “lme4” (Bates et al. 2015). Here, $\log(\text{pollen})$ is the log-transformed pollen capture per uni-ovulate flower, date is sampling date, height is maximum plant height (cm), density is a plant’s local density calculated as the inverse average distance from a focal plant to its five-nearest pollen-producing neighbours (cm^{-1}), stigma length is a flower’s stigma length, and $(1|\text{plant})$ is a random-intercept term accounting for repeated observations from the same plant within a species. Before fitting the model, I standardized the predictors date, height, density, and stigma length to z-values with mean = 0 and sd = 1 using the “scale” function from base R.

After fitting the initial full model, I performed all-subsets model selection using the “dredge” function from the package “MuMIn” (Bartoń 2023). I chose the top model as the one with the lowest AICc score. If any models within $\Delta\text{AICc} < 2$ of the top model existed, I retained them and presented them alongside the top model.

2.3.2.3 Effect of sex system on pollen capture

I tested whether pollen capture tended to be higher in hermaphroditic and monoecious species than dioecious species using a phylogenetic regression of the form $\log(\text{pollen receipt}) \sim \text{sex system}$. $\log(\text{pollen receipt})$ is the log-transformed average pollen per ovule for a species and sex system is a categorical predictor for a species’ sex system (dioecious, monoecious, or hermaphroditic). The dataset for this analysis contained 23 species, including 2 dioecious, 9 monoecious, and 12 hermaphroditic species.

I fit the PGLS model with “pgls” from the package “caper” (Orme et al. 2018), using maximum likelihood to estimate the parameter branch scaling length parameter λ . The

phylogenetic variance-covariance matrix for the 23 species used in this analysis was built using the function “phylomaker” from the package “V.PhyloMaker2” (Jin and Qian 2022) using the seed plant phylogeny GBOTB.extended.TPL (Jin and Qian 2022) and the function’s default phylogenetic hypothesis scenario, Scenario 3 (Qian and Jin 2016) (Figure B-2).

As with the analyses for pollen production and size, I also ran a linear mixed effects model with a random-intercept term for species, $\log(\text{pollen receipt}) \sim \text{sex system} + (1/\text{species})$ using “lmer” (Bates et al. 2015). I calculated the estimated marginal means for pollen receipt for each sex system using “emmeans” (Lenth 2023), and used a Tukey’s HSD post-hoc test to test for pairwise differences in pollen size between the different sex systems.

2.3 Pollination efficiency

I calculated pollination efficiency as pollen transfer efficiency (PTE) for 19 species, including 2 dioecious, 8 monoecious, and 9 hermaphroditic species, where I define PTE as

$$PTE = \frac{\text{pollen receipt per flower}}{\text{pollen production per flower}} \times 100\%.$$

Pollen receipt per ovule is the average pollen receipt per uni-ovulate flower for a given species and pollen production per anther is the average per-flower pollen production for a given species. When total flower pollen production was not available, I calculated an estimated value by multiplying measurements of pollen per anther by the average stamen number per flower for each species.

Chapter 3

Results

3.1 Pollen production and pollen size

3.1.1 Summary

Pollen production varied across the 31 wind-pollinated species (Table 3-1). Mean pollen production per anther ranged from as few as 169 ± 64 (mean \pm sd) grains/anther in the sedge *Scirpus microcarpus* (Cyperaceae) to as many as 7802 ± 2754 in the grass *Leymus innovatus* (Poaceae), representing over a 38-fold difference between the most extreme species (Table 3-1). Within-species variability in pollen production, measured as the coefficient of variation for pollen production per anther, ranged from as small as $CV = 7\%$ in the grass *Agrostis stolonifera* (Poaceae) to as much as 84% in the grass *Festuca rubra* (Poaceae).

Pollen size, measured as pollen diameter, also varied across species. The smallest pollen was found in the dioecious herb *Thalictrum dioicum* (Ranunculaceae) at 16.6 ± 0.6 (μm) and the largest pollen was found in the grass *Elymus trachycaulus* (Poaceae), at 37.7 ± 1.6 (μm) (Table 3-1). Within species, pollen size was least variable in the grass *Agrostis stolonifera* (Poaceae) ($CV = 0.3\%$) and most variable in the grass *Hierochloa odorata* ($CV = 8.4\%$).

For all 31 species, variability in pollen size was an order of magnitude smaller than variability in pollen production, as measured through CV values for pollen diameter and production per anther. Overall, the CVs for pollen size were significantly less than those of pollen production per anther across species (paired t-test: $t_{29}=11.0$, $p\text{-value}=\leq 0.001$).

3.1.2 Within-species pollen size-number tradeoff

For most species, there was no significant relationship between pollen volume and number (Table 3-2, Figure 3-1). However, in 6 of 23 species, I found individuals that made larger pollen grains also made fewer grains per anther. In just one species, *Leymus innovatus* (Poaceae), a hermaphroditic grass, individuals with larger pollen made significantly more pollen (Table 3-2). In *Ambrosia artemisiifolia*, *Bromus inermis*, *Carex hirtifolia*, *Chenopodium album*, *Festuca pratensis*, and *Koeleria cristata*, pollen size had a significant, negative relationship with pollen number, indicating a potential pollen size-number trade-off in these species (Table 3-2). Of the species where evidence for a within-species size-number tradeoff was bound, *Bromus inermis*, *Festuca pratensis*, and *Koeleria cristata* are all hermaphroditic grasses (Poaceae); *Ambrosia artemisiifolia* is a monoecious herb (Asteraceae); *Carex communis* is a monoecious sedge (Cyperaceae); and *Chenopodium album* is a hermaphroditic herb (Amaranthaceae).

3.1.3 Influence of sex system on pollen production

I modelled how sex system impacts pollen production using phylogenetic least squares (PGLS) to control for phylogenetic relatedness between species and using a term for pollen volume to control for a pollen size-number relationship ($\log(\text{pollen production per anther}) \sim \log(\text{pollen volume}) + \text{sex system}$). The maximum-likelihood estimate for λ , the model's branch length scaling parameter, was 0, equivalent to a model with no phylogenetic structure in the data ($\hat{\lambda}_{\text{ML}} = 0$, $p\text{-value}_{\lambda=0} = 1$, $p\text{-value}_{\lambda=1} < 0.001$). This suggests that species' phylogenies had little impact on pollen production. Since there was no evidence of phylogenetic structure in the data, I used a linear mixed effects model with a random-slope term for pollen volume to model the relationship between pollen production and sex system while accounting for correlations between pollen production and pollen size. While the PGLS model can only take in species-level means as input, the linear mixed-effects model can be run on individual-level data, allowing it to

better account for within-species variation in pollen production than a PGLS model with $\lambda=0$ (equivalent to running an ordinary least squares model). I included a random-slope term for pollen volume to account for species potentially having different pollen size-number relationships ($\log(\text{pollen production per anther}) \sim \log(\text{pollen volume}) + \text{sex system} + (\log(\text{pollen volume})/\text{species})$). I compared this model to one with a random-intercept term for species using the *anova()* function and found that the random-slope model explained significantly more variation in pollen production at $\alpha=0.05$. From this random-slope model, sex system ($F_{2,21.6} = 4.24$, p -value = 0.03) but not pollen volume ($\hat{\beta}_{\log \text{ pollen volume}} = -0.24$, $SE_{\log \text{ pollen diameter}} = 0.21$, $F_{1,19.9} = 1.25$, p -value = 0.27) had a significant effect on pollen production. The negative estimate for pollen volume suggests some evidence for a between-species pollen-size number tradeoff, where species that make larger pollen also tend to make fewer pollen grains. A post-hoc Tukey's HSD test showed that hermaphroditic species produced significantly more pollen than monoecious species, while pollen production in dioecious species did not differ significantly from that of monoecious or hermaphroditic species (Tukey's HSD, contrast D-M: p -value = 0.55, D-H: p -value = 0.96, M-H: p -value = 0.03; Figure 3-2).

3.1.4 Effect of sex system on pollen size

I first tested whether sex system impacts a species' pollen size by using a PGLS model to control for phylogenetic relatedness between species ($\text{pollen diameter} \sim \text{sex system}$). The maximum-likelihood estimate for the branch-length scaling parameter was $\lambda = 0.99$, which was significantly different from 0 (p -value = 0.03) but not 1 (p -value = 0.13), suggesting that more closely related species tended to have similar pollen sizes. From this model, sex system did not have a significant effect on pollen size ($F_{2,28} = 0.61$, p -value = 0.55). I also ran a similar mixed effects model on individual-level data with a random intercept term for species (pollen diameter

$\sim \text{sex system} + (1/\text{species})$. Under the linear mixed effects model, sex system did have a significant impact on pollen size ($F_{2,20.0} = 7.14$, $p\text{-value} = 0.0046$). A post-hoc Tukey's HSD test showed that dioecious species had significantly smaller pollen than hermaphroditic species but monoecious species' did not produce pollen that was significantly larger or smaller than that of dioecious or hermaphroditic species (Tukey's HSD, contrast D-M: $p\text{-value} = 0.33$, contrast D-H: $p\text{-value} = 0.014$, contrast M-H: $p\text{-value} = 0.031$; Figure 3-3).

Table 3-1. Summary of pollen size (pollen diameter, μm) and number (pollen per anther) for 31 wind-pollinated flowering plant species. For the column “Sex system”, D = dioecious, M = monoecious, H = hermaphroditic. The number of individuals measured per species is listed as N.

Species	Family	Sex system	N	Pollen size (μm)				Pollen per anther			
				Mean \pm SD	CV (%)	Min	Max	Mean \pm SD	CV (%)	Min	Max
<i>Agrostis stolonifera</i>	Poaceae	H	4	24.8 \pm 0.1	0.3%	24.75	24.90	2347 \pm 159	6.8%	2162	2549
<i>Amaranthus retroflexus</i>	Amaranthaceae	M	16	24.7 \pm 1.7	6.8%	21.92	28.15	2648 \pm 618	23.4%	1467	3733
<i>Ambrosia artemisiifolia</i>	Asteraceae	M	19	17.9 \pm 0.4	2.1%	17.44	19.03	741 \pm 391	52.7%	228	1532
<i>Avenula hookeri</i>	Poaceae	H	5	28.1 \pm 1.6	5.7%	25.88	29.73	1719 \pm 1078	62.7%	771	3491
<i>Bromus carinatus</i>	Poaceae	H	3	32.6 \pm 0.2	0.6%	32.39	32.77	5216 \pm 1212	23.2%	3887	6261
<i>Bromus inermis</i>	Poaceae	H	30	33.5 \pm 2.6	7.7%	30.10	40.41	5659 \pm 2452	43.3%	940	11633
<i>Carex communis</i>	Cyperaceae	M	16	25 \pm 0.8	3.3%	23.20	26.11	618 \pm 88	14.3%	507	776
<i>Carex hirtifolia</i>	Cyperaceae	M	18	25.2 \pm 0.4	1.6%	24.67	26.07	665 \pm 152	22.9%	365	950
<i>Carex pedunculata</i>	Cyperaceae	M	18	24.6 \pm 0.7	3.0%	23.23	25.97	525 \pm 126	24.0%	335	909
<i>Carex plantaginea</i>	Cyperaceae	M	4	27 \pm 0.2	0.7%	26.75	27.23	1006 \pm 115	11.4%	872	1129
<i>Carex stipata</i>	Cyperaceae	M	35	24.6 \pm 0.8	3.1%	23.81	26.70	415 \pm 73	17.6%	256	568
<i>Chenopodium album</i>	Amaranthaceae	H	22	24.2 \pm 0.6	2.3%	23.27	25.45	525 \pm 137	26.2%	273	824
<i>Elymus repens</i>	Poaceae	H	33	37.1 \pm 1.6	4.2%	33.84	39.19	4995 \pm 1848	37.0%	1481	8909
<i>Elymus trachycaulus</i>	Poaceae	H	10	37.7 \pm 1.6	4.1%	34.91	39.23	5395 \pm 927	17.2%	3249	6493
<i>Festuca campestris</i>	Poaceae	H	60	28.9 \pm 1.6	5.4%	23.92	32.58	6518 \pm 1947	29.9%	1084	10865
<i>Festuca pratensis</i>	Poaceae	H	14	29.6 \pm 1.1	3.8%	27.82	31.11	2473 \pm 931	37.7%	1095	4481
<i>Festuca rubra</i>	Poaceae	H	8	29.1 \pm 1.2	4.1%	26.63	30.51	3037 \pm 2565	84.4%	649	7500
<i>Hierochloe odorata</i>	Poaceae	H	50	22.6 \pm 1.9	8.4%	18.08	25.58	1713 \pm 784	45.7%	51	3631
<i>Koeleria cristata</i>	Poaceae	H	25	22 \pm 1.2	5.3%	20.70	24.48	2374 \pm 1045	44.0%	866	4818
<i>Leymus innovatus</i>	Poaceae	H	35	35.2 \pm 1.6	4.7%	31.90	38.18	7802 \pm 2754	35.3%	3737	15584
<i>Phalaris arundinacea</i>	Poaceae	H	7	32.1 \pm 0.5	1.6%	31.08	32.53	1496 \pm 493	32.9%	532	2106
<i>Phleum pratense</i>	Poaceae	H	30	29.9 \pm 1.8	6.0%	26.82	33.46	1697 \pm 595	35.1%	265	2654
<i>Plantago lanceolata</i>	Plantaginaceae	H	24	21.2 \pm 1.2	5.6%	18.59	23.16	2749 \pm 768	28.0%	1009	4743
<i>Poa juncifolia</i>	Poaceae	H	6	21.7 \pm 1	4.6%	20.02	22.99	2426 \pm 1037	42.7%	1320	4195

<i>Poa secunda</i> subsp. <i>secunda</i>	Poaceae	H	3	23.4 ± 0.4	1.9%	22.90	23.67	923 ± 413	44.7%	575	1379
<i>Rumex acetosella</i>	Polygonaceae	D	21	20 ± 0.6	3.0%	19.30	21.49	2070 ± 564	27.3%	1034	3242
<i>Rumex crispus</i>	Polygonaceae	M	20	24.1 ± 0.6	2.3%	23.05	24.85	758 ± 166	21.9%	499	1103
<i>Schizachne</i> <i>purpurascens</i>	Poaceae	H	12	29.3 ± 0.5	1.7%	28.61	30.25	287 ± 99	34.6%	150	430
<i>Scirpus microcarpus</i>	Cyperaceae	M	14	22.8 ± 0.4	1.9%	21.97	23.44	169 ± 64	37.7%	109	334
<i>Stipa columbiana</i>	Poaceae	H	10	28.5 ± 1.3	4.7%	26.52	30.09	673 ± 387	57.5%	144	1336
<i>Thalictrum dioicum</i>	Ranunculaceae	D	23	16.6 ± 0.6	3.7%	15.88	17.71	3320 ± 1295	39.0%	1108	5450

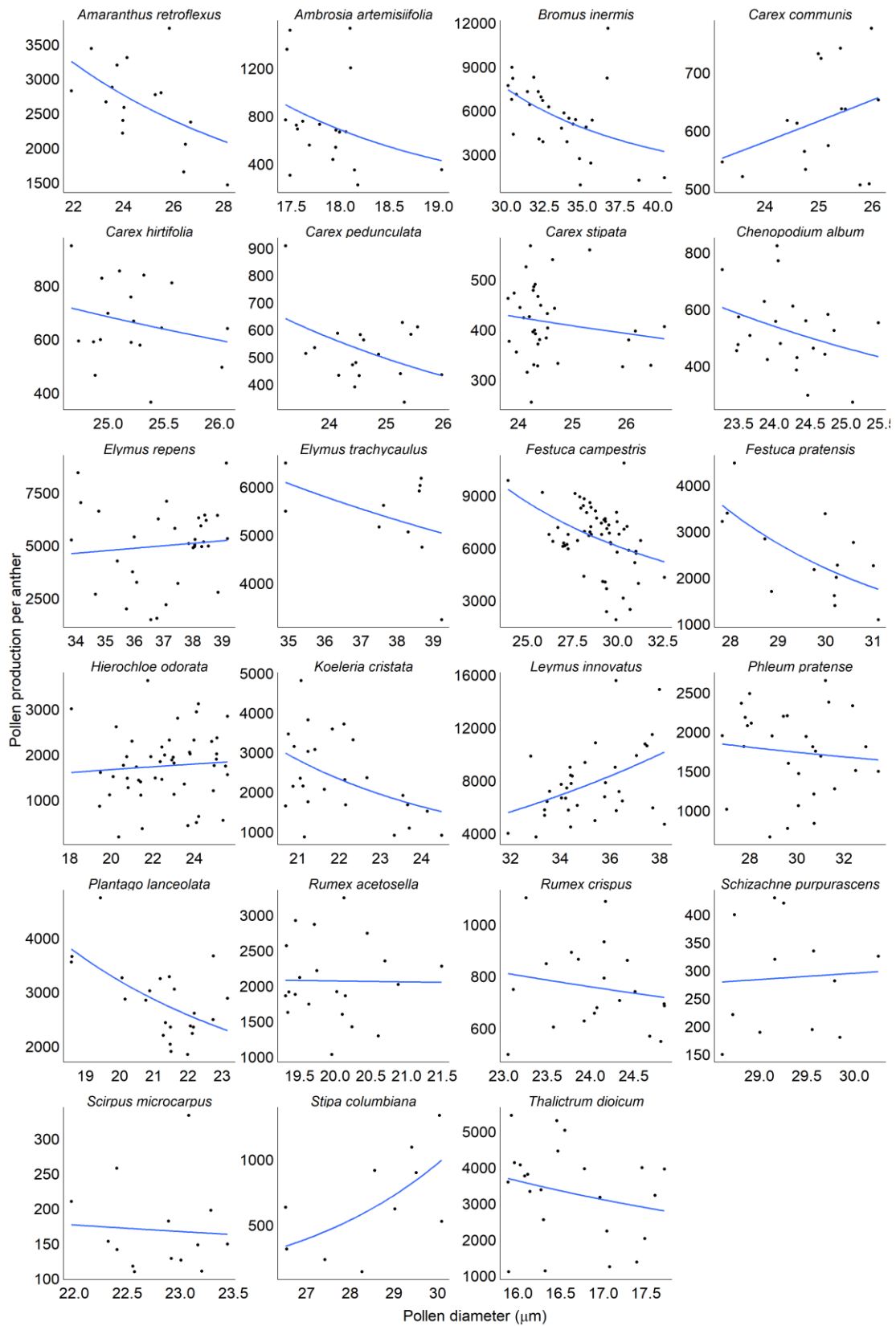


Figure 3-1. Relationship between pollen production per anther and pollen diameter for 23 wind-pollinated flowering plant species. Line of best fit shown in blue. Statistical details are shown in Table 3-2.

Table 3-2. Summary of linear regression models predicting pollen production by size as $\log(\text{pollen per anther}) \sim \log(\text{pollen volume})$ for each of 23 wind-pollinated flowering plant species. The regression slope represents the exponent a in the relationship $\log(n) = \log(cs^a)$, where n is the number of pollen grains per anther, s is pollen grain volume, and c is a constant. For the column “Sex system”, D = dioecious, M = monoecious, H = hermaphroditic. Significant p -values (<0.05) for the slope of pollen volume are bolded. See Figure 3-1 for depictions of the data and the regression line.

Species	Sex system	Term	Estimate	SE	df	t	p -value
<i>Amaranthus retroflexus</i>	M	Intercept	14.72	2.40	14	6.13	<0.001
		Volume	-0.77	0.27	14	-2.86	0.01
<i>Ambrosia artemisiifolia</i>	M	Intercept	31.52	15.04	17	2.10	0.05
		Volume	-3.13	1.88	17	-1.66	0.11
<i>Bromus inermis</i>	H	Intercept	23.36	4.03	28	5.79	<0.001
		Volume	-1.50	0.41	28	-3.68	<0.001
<i>Carex communis</i>	M	Intercept	2.18	3.21	14	0.68	0.51
		Volume	0.47	0.36	14	1.32	0.21
<i>Carex hirtifolia</i>	M	Intercept	16.52	11.50	16	1.44	0.17
		Volume	-1.11	1.27	16	-0.87	0.4
<i>Carex pedunculata</i>	M	Intercept	14.16	5.22	16	2.71	0.02
		Volume	-0.88	0.58	16	-1.52	0.15
<i>Carex stipata</i>	M	Intercept	8.94	3.08	33	2.91	0.01
		Volume	-0.33	0.34	33	-0.95	0.35
<i>Chenopodium album</i>	H	Intercept	18.17	7.34	20	2.48	0.02
		Volume	-1.34	0.82	20	-1.63	0.12
<i>Elymus repens</i>	H	Intercept	3.95	6.43	31	0.61	0.54
		Volume	0.44	0.63	31	0.70	0.49
<i>Elymus trachycaulus</i>	H	Intercept	15.29	5.12	8	2.99	0.02
		Volume	-0.66	0.50	8	-1.31	0.23
<i>Festuca campestris</i>	H	Intercept	16.16	2.41	58	6.70	<0.001
		Volume	-0.79	0.26	58	-3.07	<0.01
<i>Festuca pratensis</i>	H	Intercept	28.39	7.15	12	3.97	<0.01
		Volume	-2.17	0.75	12	-2.89	0.01
<i>Hierochloe odorata</i>	H	Intercept	5.64	2.92	48	1.93	0.06
		Volume	0.19	0.34	48	0.58	0.56
<i>Koeleria cristata</i>	H	Intercept	21.65	4.73	23	4.57	<0.001
		Volume	-1.62	0.55	23	-2.95	0.01
<i>Leymus innovatus</i>	H	Intercept	-1.97	3.78	32	-0.52	0.61
		Volume	1.08	0.38	32	2.88	0.01

<i>Phleum pratense</i>	H	Intercept	8.53	3.70	28	2.31	0.03
		Volume	-0.12	0.39	28	-0.30	0.76
<i>Plantago lanceolata</i>	H	Intercept	13.99	2.10	22	6.65	<0.001
		Volume	-0.71	0.25	22	-2.89	0.01
<i>Rumex acetosella</i>	D	Intercept	8.22	6.10	19	1.35	0.19
		Volume	-0.07	0.73	19	-0.10	0.92
<i>Rumex crispus</i>	M	Intercept	10.74	6.39	18	1.68	0.11
		Volume	-0.47	0.72	18	-0.65	0.53
<i>Schizachne purpurascens</i>	H	Intercept	-2.76	20.87	10	-0.13	0.9
		Volume	0.88	2.20	10	0.40	0.7
<i>Scirpus microcarpus</i>	M	Intercept	9.45	14.47	12	0.65	0.53
		Volume	-0.50	1.66	12	-0.30	0.77
<i>Stipa columbiana</i>	H	Intercept	-18.46	14.31	8	-1.29	0.23
		Volume	2.63	1.52	8	1.73	0.12
<i>Thalictrum dioicum</i>	D	Intercept	14.25	7.47	21	1.91	0.07
		Volume	-0.80	0.96	21	-0.83	0.41

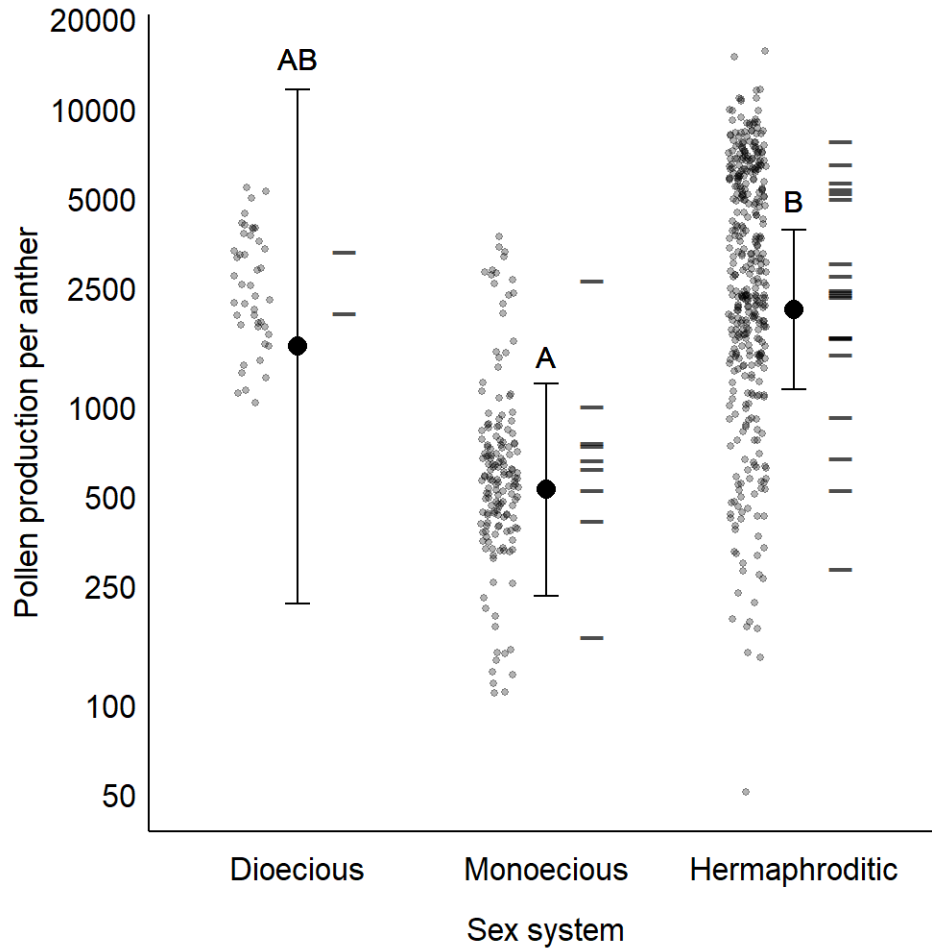


Figure 3-2. Mean pollen production per anther for dioecious (n=2), monoecious (n=9), and hermaphroditic (n=20) wind-pollinated flowering plant species. Left: Distribution of individual mean pollen production per anther. Centre: Marginal mean (back-transformed) pollen production per sex system estimated from the linear mixed effects model. Error bars are 95% CIs. Letters represent the results of a pairwise Tukey's HSD test at $\alpha=0.05$. Right: Bars represent species' mean pollen production.

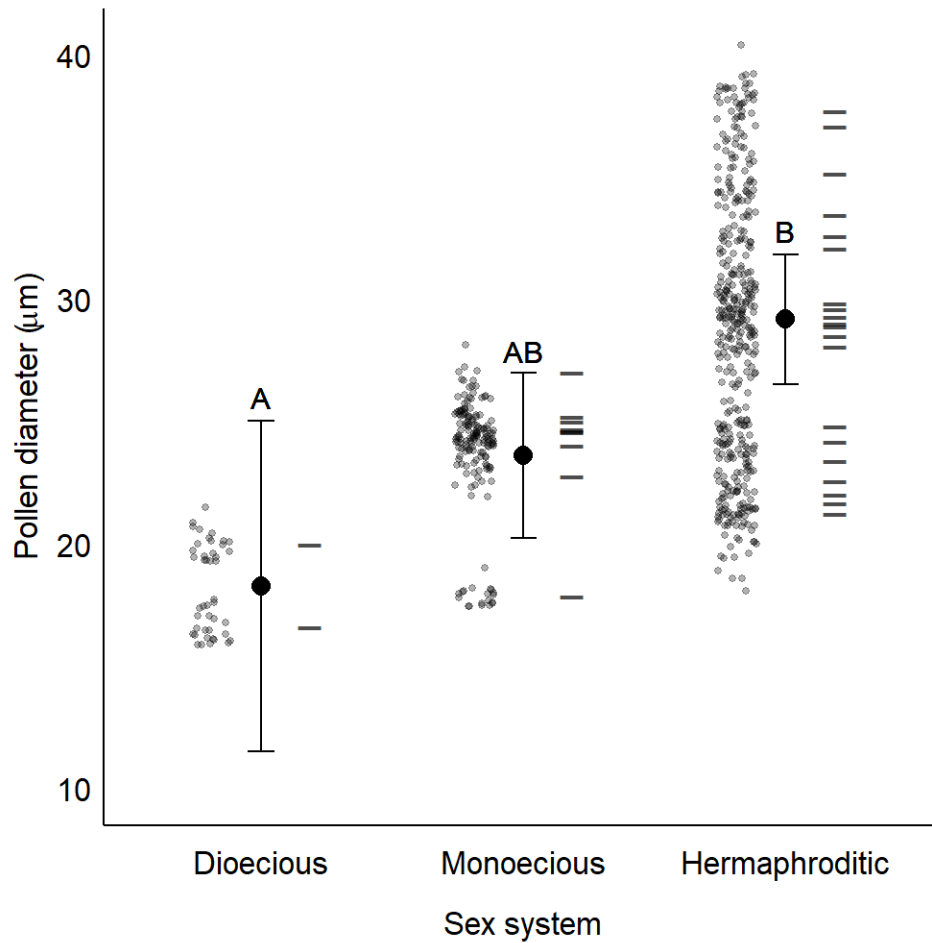


Figure 3-3. Mean pollen diameter for dioecious (n=2), monoecious (n=9), and hermaphroditic (n=20) wind-pollinated flowering plant species. Left: Distribution of individual mean pollen diameters. Centre: Marginal mean pollen size per sex system predicted from the mixed effects model. Error bars are 95% CIs. Letters represent the results of a pairwise Tukey's HSD test at $\alpha=0.05$. Right: Bars represent species mean pollen diameters.

3.2 Stigmatic pollen capture

3.2.1 Summary

Stigmatic pollen loads were measured as the number of grains per ovule, with all sampled species having a single ovule per flower, except *P. lanceolata*, which has 2. Mean pollen loads ranged from 2.27 in the dioecious herb *Rumex acetosella* (Polygonaceae) to 112.98 in the hermaphroditic grass *Schizachne purpurascens* (Poaceae) (Table 3-3). Maximum pollen capture per species ranged from as few as 11 grains per ovule in *Rumex acetosella* to as many as 2200 in *Elymus innovatus* (Poaceae) (Table 3-3). Distributions of mean stigmatic pollen load per individual varied between species (Figure 3-4). Pollen load distributions were highly right-skewed in some species, where most stigmas received zero grains or just one grain but a few received upwards of 20 (e.g. *Rumex acetosella*, *Thalictrum dioicum*). Other species' distributions peaked at values well above zero, indicating that most stigmas received more pollen than there are ovules per stigma (e.g. *Elymus innovatus*, *Plantago lanceolata*, *Setaria viridis*).

3.2.2 Individual-level effects on pollen capture

The date flowers were sampled affected pollen capture in most species (10 of 13), with later-sampled stigmas capturing more pollen than earlier-sampled stigmas in all species except *Schizachne purpurascens*, where earlier-collected stigmas received more pollen (Table 3-4, Figure B-3). A plant's height had little impact on the amount of pollen it received (Table 3-4, Figure B-4). In just 1 of 13 species, the sedge *Carex stipata* (Cyperaceae), taller plants received more pollen (Table 3-4). Density, measured as the inverse of the average distance from a focal plant to its five nearest pollen-producing neighbours, affected pollen capture in 2 species, *Carex stipata* and *Rumex acetosella* (Table 3-4, Figure B-5). In these species, pollen capture decreased

with decreased density, suggesting that plants with more pollen-producing neighbours received higher pollen loads. Notably, these three species had relatively low average pollen loads (*Carex stipata*: mean = 4.66 grains/ovule, sd = 11.6; *Rumex acetosella*: mean = 2.26 grains/ovule, sd 2.43; Table 3-4). These species also had the highest average distances from focal plants to their five-nearest pollen producing neighbours, with *Rumex acetosella* at an average distance of 331.4 cm and *Carex stipata* at 185.3 cm (Table A-4). Lastly, longer stigmas received more pollen in 9 of 13 species (Table 3-4, Figure B-6). These 9 species contained diverse members, including both dioecious species, *Rumex acetosella* (Polygonaceae) and *Thalictrum dioicum* (Ranunculaceae), as well as monoecious *Ambrosia artemisiifolia* (Asteraceae), *Rumex crispus* (Polygonaceae), *Carex communis* (Cyperaceae), *Carex hirtifolia*, and *Carex stipata*, and the hermaphroditic herbs *Chenopodium album* (Amaranthaceae) and *Plantago lanceolata* (Plantaginaceae).

3.2.3 Effect of sex system on pollen capture

When controlling for phylogeny using phylogenetic least squares, species' stigmatic pollen loads do not differ significantly between sex systems (PGLS: $pollen\ load \sim sex\ system$, $\hat{\lambda} = 0.738$ (p -value $\lambda=0 = 0.51$, p -value $\lambda=1 = 0.004$), $F_{2,20} = 2.31$, p -value = 0.125). However, since λ was not significantly different from zero, I repeated the analysis with a linear mixed effects model on individual-level data, rather than the species-level data necessarily used in the PGLS analysis. In the mixed effects model, sex system does have a significant effect on stigmatic pollen loads (linear mixed effects model: $pollen\ load \sim sex\ system + (1/species)$, $F_{2,19.9} = 8.58$, p -value = 0.002). A Tukey's HSD test shows that hermaphroditic species capture significantly more pollen than dioecious or monoecious species, but pollen capture is not significantly

different between dioecious and monoecious species (Tukey's HSD, contrast D-M: p -value = 0.38, contrast D-H: p -value = 0.003, contrast M-H: p -value = 0.003; Figure 3-5).

Table 3-3. Stigmatic pollen loads for 23 wind-pollinated species. Species' sex systems are coded as follows: D = dioecious, M = monoecious, H = hermaphroditic. N represents the number of individuals measured per species.

Species	Sex system	N	Stigmatic pollen load				
			Mean	SD	CV (%)	Min	Max
<i>Amaranthus retroflexus</i>	H	15	22.4	26.92	120%	0	150
<i>Ambrosia artemisiifolia</i>	M	15	51.03	76.92	151%	0	460
<i>Bromus inermis</i>	H	67	50.57	75.68	150%	0	645
<i>Carex communis</i>	M	22	11.29	16.15	143%	0	109
<i>Carex hirtifolia</i>	M	48	27.29	54.22	199%	0	392
<i>Carex pedunculata</i>	M	23	10.63	13.15	124%	0	66
<i>Carex plantaginea</i>	M	27	9.92	22.76	230%	0	214
<i>Carex stipata</i>	M	30	4.66	11.6	249%	0	110
<i>Chenopodium album</i>	H	30	3.09	3.73	121%	0	20
<i>Dichanthelium implicatum</i>	H	25	14.62	16.32	112%	0	79
<i>Dichanthelium linearifolium</i>	H	20	38.05	61.79	162%	0	260
<i>Elymus repens</i>	H	41	84.28	69.93	83%	5	381
<i>Festuca campestris</i>	H	83	17.89	35.74	200%	0	391
<i>Leymus innovatus</i>	H	79	107.42	195.09	182%	1	2200
<i>Phleum pratense</i>	H	22	38.79	43.61	112%	0	226
<i>Plantago lanceolata</i>	H	17	94.97	107.1	113%	0	750
<i>Plantago major</i>	H	16	112.98	96.65	86%	0	341
<i>Rumex acetosella</i>	D	25	2.26	2.43	108%	0	11
<i>Rumex crispus</i>	M	25	6.63	12.54	189%	0	134
<i>Schizachne purpurascens</i>	H	31	92.26	121.05	131%	0	645
<i>Scirpus microcarpus</i>	M	30	5.16	5.69	110%	0	38
<i>Setaria viridis</i>	H	45	57.82	37.91	66%	2	188
<i>Thalictrum dioicum</i>	D	59	3.69	6.48	175%	0	39



Figure 3-4. Distributions of pollen load for 23 wind-pollinated flowering plant species. Species' sex systems are coded as follows: D = dioecious (green), M = monoecious (blue), H = hermaphroditic (orange).

Table 3-4. Summary of results from mixed models predicting the relationship between stigmatic pollen receipt and individual-level factors for 13 wind-pollinated species. Table shows coefficients (β), standard errors, t-values, and corresponding p-values for linear models generated using model selection with dredge, from the full model $\log(\text{pollen}) \sim \text{date} + \text{height} + 1/\text{density} + \text{stigma length} + (1|\text{plant})$. When multiple models had indistinguishable explanatory power ($\Delta\text{AICc} < 2$), the fullest model was considered as the top model (bolded, when applicable).

Species	Model	AICc	Trait	β	SE	df	<i>t</i>	<i>p</i> -value
<i>Ambrosia artemisiifolia</i>	$\log(\text{pollen}) \sim 1$	622.5	Intercept	3.95	0.38	29.3	10.3	<0.001
	$\log(\text{pollen}) \sim \text{stigma length}$	623.7	Intercept	4.49	0.10	25.7	45.9	<0.001
			Stigma length	0.15	0.07	217.1	2.3	0.024
<i>Carex communis</i>	$\log(\text{pollen}) \sim \text{date} + \text{stigma length}$	553.5	Intercept	1.94	0.10	20.2	18.7	<0.001
			Date	0.55	0.06	185.9	8.7	<0.001
			Stigma length	0.20	0.07	196.0	3.1	0.002
<i>Carex hirtifolia</i>	$\log(\text{pollen}) \sim \text{stigma length}$	703.4	Intercept	2.24	0.10	22.6	22.5	<0.001
			Stigma length	0.29	0.09	197.9	3.2	0.002
<i>Carex pedunculata</i>	$\log(\text{pollen}) \sim \text{date}$	217.6	Intercept	1.91	0.18	11.7	10.7	<0.001
			Date	0.78	0.09	70.0	8.4	<0.001
<i>Carex plantaginea</i>	$\log(\text{pollen}) \sim \text{date}$	260.5	Intercept	1.47	0.16	18.1	9.1	<0.001
			Date	0.27	0.09	86.8	3.1	0.003
<i>Carex stipata</i>	$\log(\text{pollen}) \sim \text{date} + \text{density} + \text{stigma length}^*$	902.4	Intercept	0.98	0.05	316.0	18.5	<0.001
			Date	0.25	0.05	316.0	4.6	<0.001
			1/Density	0.16	0.05	316.0	2.9	0.004
			Stigma length	0.26	0.05	316.0	4.9	<0.001
	$\log(\text{pollen}) \sim \text{date} + \text{height} + \text{density} + \text{stigma length}^*$	903	Intercept	0.98	0.05	315.0	18.6	<0.001
			Date	0.25	0.05	315.0	4.7	<0.001
			Height	0.13	0.05	315.0	2.3	0.020
			1/Density	0.14	0.05	315.0	2.5	0.012
$\log(\text{pollen}) \sim \text{date} + \text{height} + \text{stigma length}^*$	903.2	Intercept	0.98	0.05	316.0	18.4	<0.001	
		Date	0.25	0.05	316.0	4.6	<0.001	
		Height	0.15	0.05	316.0	2.8	0.006	
		Stigma length	0.23	0.06	316.0	4.1	<0.001	
<i>Chenopodium album</i>	$\log(\text{pollen}) \sim \text{stigma length}^*$	360.9	Intercept	1.06	0.06	147.0	16.7	<0.001

			Stigma length	0.30	0.06	147.0	4.7	<0.001
<i>Plantago lanceolata</i>	log(pollen) ~ date + stigma length	905.6	Intercept	3.61	0.12	27.4	30.1	<0.001
			Date	0.52	0.07	255.1	7.0	<0.001
			Stigma length	0.39	0.08	257.1	4.7	<0.001
<i>Rumex acetosella</i>	log(pollen) ~ date + stigma length	488.1	Intercept	0.91	0.06	28.0	14.3	<0.001
			Date	0.34	0.04	245.1	8.5	<0.001
			Stigma length	0.11	0.04	256.2	3.1	0.002
	log(pollen) ~ date + density + stigma length	489.3	Intercept	0.90	0.06	26.4	15.3	<0.001
			Date	0.32	0.04	242.9	8.0	<0.001
			1/Density	0.12	0.05	38.2	2.3	0.029
			Stigma length	0.13	0.04	254.0	3.4	0.001
<i>Rumex crispus</i>	log(pollen) ~ stigma length	495.6	Intercept	1.47	0.10	22.2	15.0	<0.001
			Stigma length	0.32	0.07	176.9	4.5	<0.001
	log(pollen) ~ date + stigma length	496.9	Intercept	1.48	0.10	21.7	14.3	<0.001
			Date	0.15	0.07	175.9	2.1	0.036
			Stigma length	0.30	0.07	175.1	4.2	<0.001
<i>Schizachne purpurascens</i>	log(pollen) ~ date	907.2	Intercept	3.63	0.12	29.4	30.2	<0.001
			Date	-				
<i>Scirpus microcarpus</i>	log(pollen) ~ date*	643.3	Intercept	1.43	0.06	23.9	22.1	<0.001
			Date	0.51	0.05	244.7	11.0	<0.001
<i>Thalictrum dioicum</i>	log(pollen) ~ date	248.6	Intercept	1.98	0.08	17.6	24.0	<0.001
			Date	0.29	0.07	97.2	4.4	<0.001
	log(pollen) ~ date + stigma length	249.6	Intercept	1.99	0.10	13.7	19.9	<0.001
			Date	0.29	0.06	89.1	4.6	<0.001
			Stigma length	0.19	0.07	95.0	2.5	0.014

*boundary (singular) fit

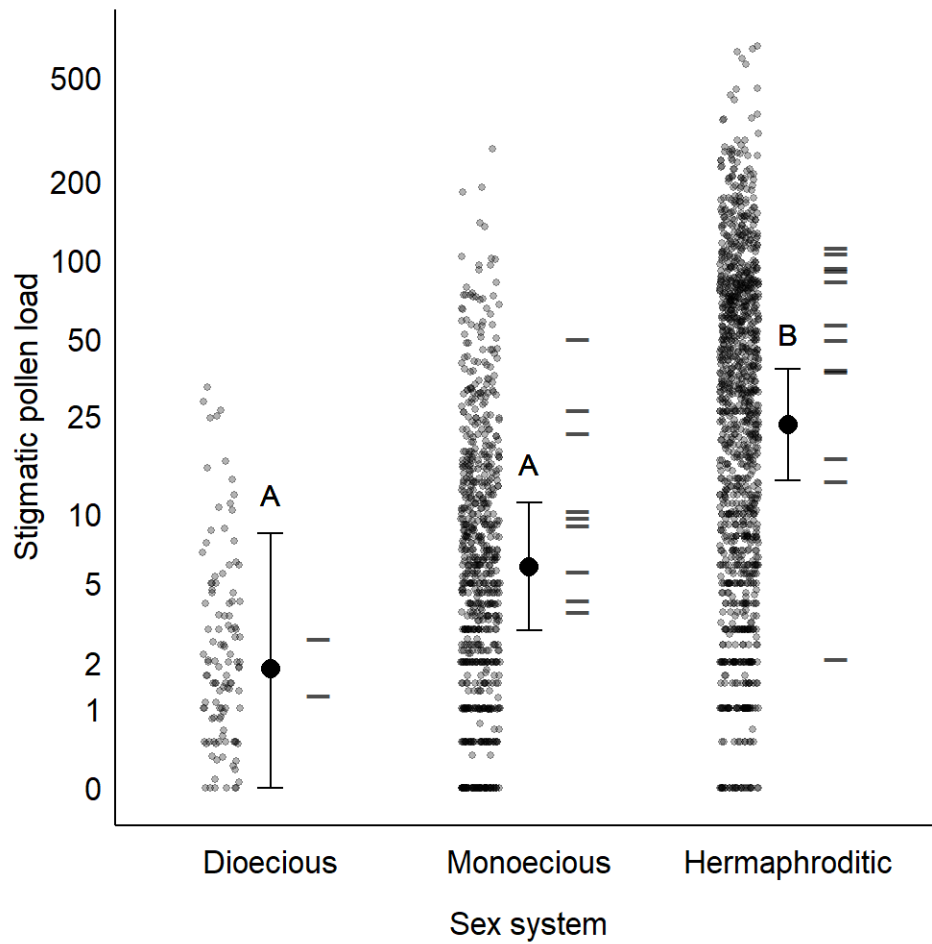


Figure 3-5. Mean stigmatic pollen loads for dioecious (n=2), monoecious (n=9), and hermaphroditic (n=12) species. Left: Distribution of individual mean stigmatic pollen loads, with species pooled within sex systems. Centre: Marginal mean pollen loads per sex system predicted from the mixed effects model. Error bars are 95% CIs. Letters represent the results of a pairwise Tukey's HSD test at $\alpha=0.05$. Right: Bars represent mean pollen loads per species.

3.3 Pollination efficiency

Pollen transfer efficiency (PTE), measured as the percentage of pollen captured to pollen produced per flower, was lowest in the two dioecious species, at 0.005% in *Thalictrum dioicum* (Ranunculaceae) and 0.02% *Rumex acetosella* (Polygonaceae) (Figure 3-6, Figure 3-7, Table 3-5) and highest in the hermaphroditic grass, *Schizachne purpurascens* (Poaceae), at an exceptional 10.7% (Table 3-5). The exceptionally high PTE in *S. purpurascens* could be related to its mating system if most of the pollen it captures is self-pollen. Both its high average pollen capture, at 92.3 grains per stigma, and low pollen production, the 2nd-lowest with an average of just 287 grains per anther and 861.5 grains per flower, are consistent with a selfing syndrome (Table 3-5). Additionally, *S. purpurascens* was one of the few species where neither density, stigma length, nor height significantly influenced pollen loads, which would also be consistent with *S. purpurascens* being primarily self-pollinating. The next highest PTE was 1.38% in *Ambrosia artemisiifolia* (Asteraceae), a monoecious, self-incompatible herb.

Table 3-5. Pollination efficiency for 19 wind-pollinated flowering plant species. Pollination efficiency is calculated as mean pollen production per flower/mean stigmatic pollen load × 100%.

Species	Sex system	Stigmatic pollen load		Pollen per flower		Pollination efficiency (%)
		Mean	SD	Mean	SD	
<i>Amaranthus retroflexus</i>	M	22.4	26.9	13241.7	3092.2	0.17%
<i>Ambrosia artemisiifolia</i>	M	51.0	76.9	3707.3	1955.4	1.38%
<i>Bromus inermis</i>	H	50.6	75.7	16976.2	7355.1	0.30%
<i>Carex communis</i>	M	11.3	16.1	1854.1	265.4	0.61%
<i>Carex hirtifolia</i>	M	27.3	54.2	1994.1	456.5	1.37%
<i>Carex pedunculata</i>	M	10.6	13.2	1573.6	377.7	0.68%
<i>Carex plantaginea</i>	M	9.9	22.8	3018.8	345.0	0.33%
<i>Carex stipata</i>	M	4.7	11.6	1245.6	219.6	0.37%
<i>Chenopodium album</i>	H	3.1	3.7	2627.3	687.1	0.12%
<i>Elymus repens</i>	H	84.3	69.9	14985.7	5545.1	0.56%
<i>Festuca campestris</i>	H	17.9	35.7	19554.4	5841.4	0.09%
<i>Phleum pratense</i>	H	38.8	43.6	5089.5	1786.0	0.76%
<i>Plantago lanceolata</i>	H	95.0	107.1	10994.6	3073.2	0.86%
<i>Rumex acetosella</i>	H	2.3	2.4	12422.7	3385.8	0.02%
<i>Rumex crispus</i>	D	6.6	12.5	4545.4	996.9	0.15%
<i>Schizachne purpurascens</i>	M	92.3	121.0	861.5	298.3	10.7%
<i>Scirpus microcarpus</i>	H	5.2	5.7	507.0	191.0	1.02%
<i>Thalictrum dioicum</i>	M	3.7	6.5	79161.6	34338.2	0.005%

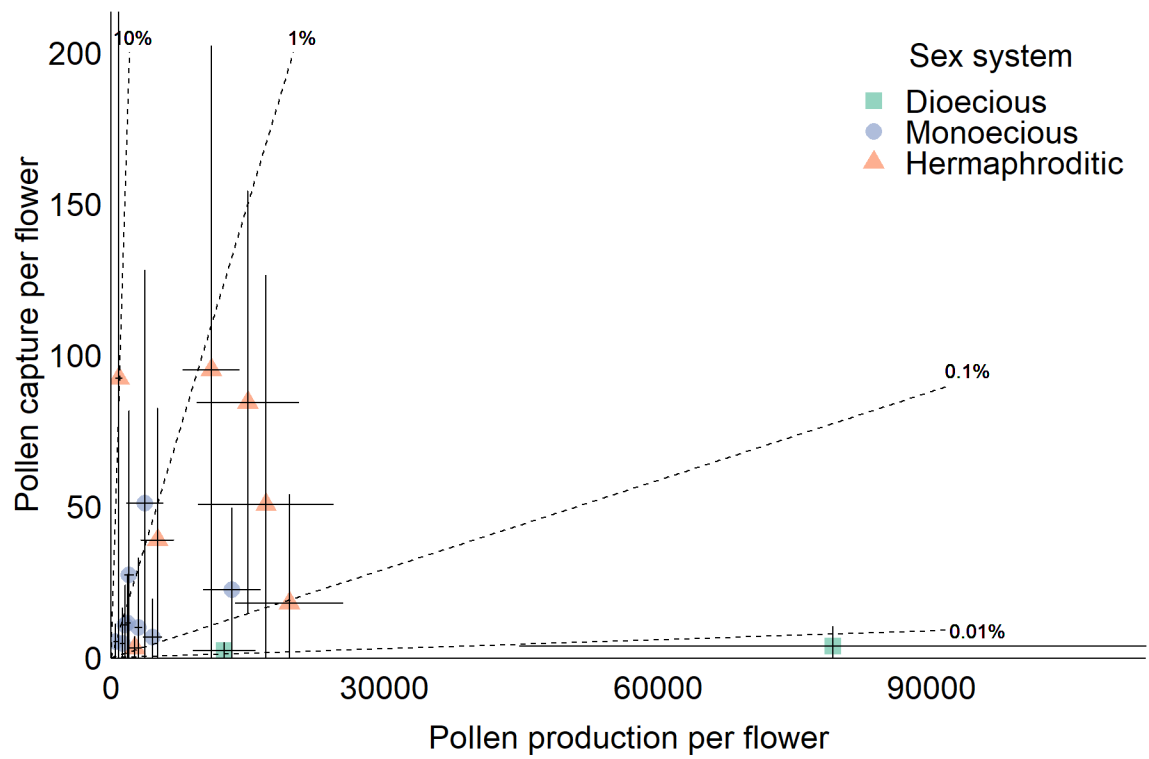


Figure 3-6. The relationship between pollen production per flower and pollen capture per stigma for 19 wind-pollinated species. Error bars are standard deviations. Dotted lines represent 0.01%, 0.1%, 1%, and 10% pollen capture efficiency.

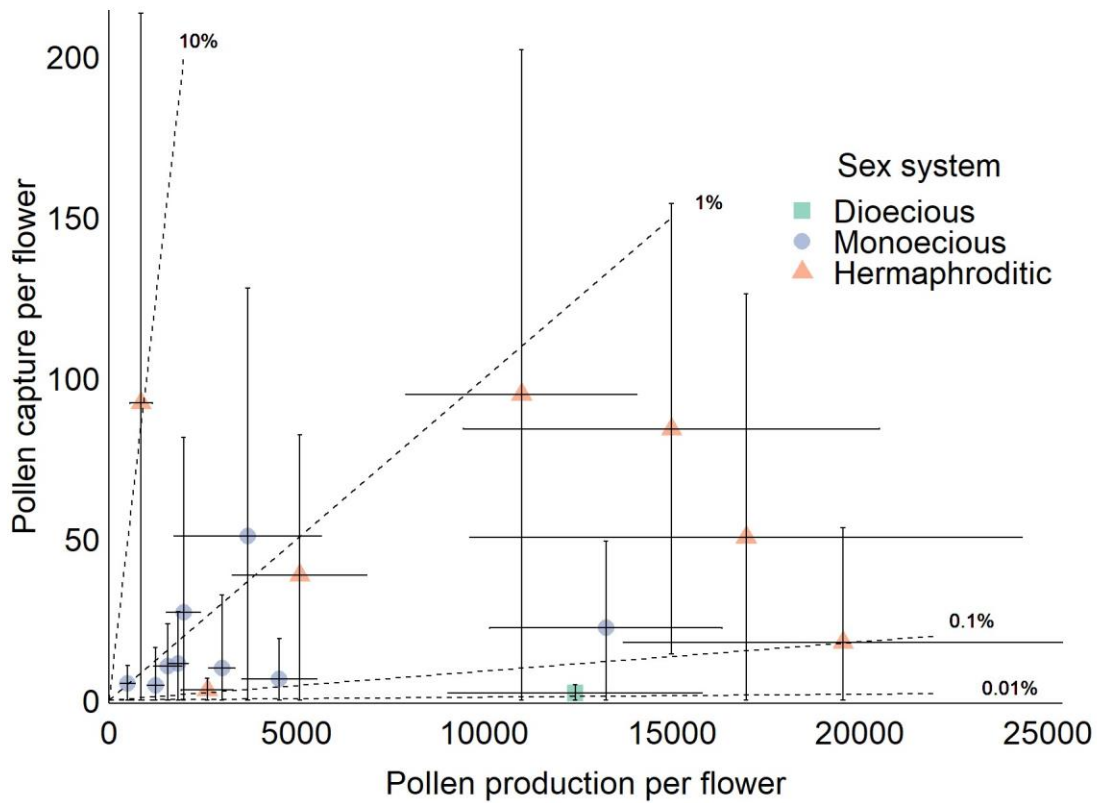


Figure 3-7. The relationship between pollen production per flower and pollen capture per stigma for 18 wind-pollinated species, *Thalictrum dioicum* excluded for better resolution between species. Error bars are standard deviations. Dotted lines represent 0.01%, 0.1%, 1%, and 10% pollen capture efficiency.

Chapter 4

Discussion

The idea that wind pollination is imprecise and wasteful as a pollination system has been prevalent throughout the literature (Meeuse 1961, Faegri and Van der Pijl 1979, Ackerman 2000). But it seems unlikely that such a widespread strategy would evolve repeatedly if most of its features were compensation mechanisms for unavoidably poor pollination. Mostly, cases for the inefficiency of wind pollination contrast the high pollen production typical of wind-pollinated plants with their low ovule production, citing both as mitigation strategies for high pollen losses and low probability of successful pollen receipt (Cruden 1977, 2000, Faegri and Van der Pijl 1979). While stochasticity and risk in pollination success from both male and female perspectives likely shape the evolution of pollen and ovule number in wind-pollinated species, wind pollination is not necessarily riskier for pollen transfer or receipt than animal-pollination. Pollen transfer efficiencies were similar to those reported for animal-pollinated species and average pollen loads exceeded ovule number for all species. Pollen production per anther and pollen capture per ovule were influenced by several factors. Sex system affected both pollen production and capture, with hermaphroditic species producing significantly more pollen per anther than monoecious species and capturing significantly more pollen per carpel than monoecious or dioecious species. Pollen size (volume) and number were negatively correlated in 6 of 23 species. Pollen diameter was significantly less variable than pollen number, suggesting it may be under stronger balancing selection. Longer stigmas and later-sampled stigmas bore higher pollen loads. Increased density of pollen-producers increased pollen capture only in the species where density was the lowest. A plant's height had little impact on its pollen capture.

Here, I will discuss the factors that contribute to variability in pollen production and capture and how these likely influence the evolution of low ovule number and high pollen production in wind-pollinated plants.

4.1 Allocation to male reproduction

One of the primary arguments for high pollen production in wind-pollinated plants is that plants overproduce pollen to secure pollination success because of the exceedingly small chance of a given pollen grain reaching a stigma (e.g. Meeuse 1961, Faegri and Van der Pijl 1979). However, pollen loss during transport may not be much greater in wind pollination than in animal pollination. Pollen transfer efficiency (PTE), the percentage of pollen captured per flower relative to the pollen produced per flower, ranges from 0.01% to 20% in animal-pollinated plants with granular pollen, with most values under 1% (Harder 2000, Harder and Johnson 2023). This is not much greater than the range I found for the 19 wind-pollinated species studied here, from 0.005% in the dioecious species *Thalictrum dioicum* to 10.7% in *Schizachne purpurascens* (Table 3-5). However, *S. purpurascens* is likely highly selfing and its PTE may not be comparable to other, primarily outcrossed species. The next highest PTE was 1.38%, in *Ambrosia artemisiifolia*. The similarity in PTE between wind- and animal-pollinated species challenges the idea that wind pollination is inefficient and suggests there may be alternative explanations for the high pollen production in wind-pollinated plants relative to their low ovule number. Important to note, however, is that my measure of PTE differed from that of Harder and Johnson (2023) and Harder (2000) in how pollen production was calculated. Their measure of PTE considered pollen production as the number of grains produced per flower that were subsequently removed from stigmas, while my measure only considered the total number of grains produced per flower. Pollen removal in wind-pollinated species requires sufficiently high

wind speeds to free pollen from anthers. Many wind-pollinated species have adaptations to maximize pollen removal, so we might expect pollen removal failure to be relatively low in wind-pollinated species. However, wind-pollinated plants may still experience pollen removal failure if wind speeds are not sufficient. The frequency and extent of pollen removal failure likely depends on a plant's environment. Complete pollen removal may be more likely in wide-open, gusty environments. For example, 29.4% of pollen remained in anthers after flowering in the woodland grass *Elymus innovatus*, while 6.5% remained in anthers of the pasture grass *Bromus inermis* (Harder 2000). Given the possibility of pollen removal failure, my estimates of PTE for wind-pollinated species may be underestimates compared to the values reported for animal-pollinated species (Harder 2000, Harder and Johnson 2023), underscoring the relative effectiveness of wind pollination further.

Risk and stochasticity may still play important roles in shaping differences in pollen production among wind-pollinated species. If plants invest in reproductive functions in proportion to the risk that those functions will limit reproductive success (Schreiber et al. 2015), then a high risk of pollen loss should select for high pollen production, so long as seed production is primarily pollen-limited, rather than resource-limited (Harder and Johnson 2023). In line with this reasoning, Harder and Johnson (2023) observed that (animal-pollinated) species with higher pollen transport efficiency (PTE) produced fewer pollen grains per flower, suggesting that species with riskier pollen transport tend to have higher pollen production. Correspondingly, (animal-) pollinator-dependent plants produced more pollen than autogamous plants (Harder and Johnson 2023). This tendency for pollen production to be higher in species with more uncertain pollen transfer may explain the differences I observed in pollen production between species of different sex systems.

Sex system may influence pollen production through both resource allocation and spatial consequences of the separation of sexes. Since hermaphroditic species produce cosexual flowers, they must allocate a portion of their reproductive resources to producing structures for both sex roles in addition to producing gametes, while unisexual flowers need only invest in structures for one sex (Heath 1977). Therefore, given the same investment in reproduction, monoecious and dioecious species with unisexual flowers may be able to produce more gametes per flower than hermaphrodites. Additionally, dioecious species likely experience greater risk in reproductive success, as they cannot self-pollinate and not all neighbours are potential mates. Given this, I expected pollen production to be highest in dioecious species and lowest in the hermaphroditic species, as has been observed in comparative analyses of herbaceous wind-pollinated species (Michalski and Durka 2009, 2010). However, I found that pollen production was high in both hermaphroditic and dioecious species compared to monoecious species, though only hermaphroditic species made significantly more pollen than the monoecious species (Figure 3-2). While this was unexpected, it might be explained by differences in mating system between the species included in my analysis. Five of the nine monoecious species were *Carex* sedges, which are likely largely selfing (e.g. Friedman and Barrett 2009). Patterns of pollen production and capture in these species were consistent with a selfing syndrome, where pollen production was relatively low, ranging from 525 to 1006 grains per anther (Table 3-1), and pollen capture was relatively high, ranging from 4.7 to 27.3 grains per uniovulate flower (Table 3-3). In contrast, the top three pollen producers, each with an average pollen production of above 5500 grains/anther, were strongly outcrossing hermaphroditic species, including *Leymus innovatus* (Dewey 1983), *Festuca campestris* (Mengli et al. 2008) and *Bromus inermis* (McKone 1987). Therefore, the significantly higher pollen production in hermaphroditic species may be more related to

differences in mating system between the hermaphroditic and monoecious species sampled than to their sex systems alone. Additionally, unevenness in the sample sizes of species within each sex system may have influenced the results of the comparison between sex systems. Only two dioecious species were included in the analysis, compared to nine monoecious and 20 hermaphroditic species. While dioecy is relatively uncommon in the flowering plants, present in around 4% of all species, it is found in approximately 30% of wind-pollinated flowering plants (Renner 2014). Therefore, while dioecious species are relatively rare, they are still likely underrepresented in this sample of species.

If pollen size and number are correlated, pollen production may also be influenced by selection on pollen size. I found statistically significant evidence for a negative correlation between pollen volume and number in six of 23 species, *Ambrosia artemisiifolia*, *Bromus inermis*, *Carex hirtifolia*, *Chenopodium album*, *Festuca pratensis*, and *Koeleria cristata* (Table 3-2). These species were from various families and sex systems, including the Asteraceae, Poaceae, Cyperaceae, and Amaranthaceae, suggesting that this was not a trait unique to any one family. In one species, *Leymus innovatus*, pollen volume and number were significantly positively correlated (Table 3-2). Many of these species had coefficients of variation (CV) for pollen per anther greater than the across-species average (34.2%), including *A. artemisiifolia* (CV=52.4%), *B. inermis* (43.3%), *F. pratensis* (37.7%), *K. cristata* (32.9%), and *L. innovatus* (35.3%) as well as CVs for pollen diameter greater than the average CV (3.7%), including *B. inermis* (7.7%), *F. pratensis* (3.8%), *K. cristata* (5.3%), and *L. innovatus* (4.7%), and sample sizes of at least 14 (Table 3-1). For the remaining species, some had sample sizes that were likely too small to provide enough power to detect a correlation between pollen size and number, e.g.,

Agrostis stolonifera, *Avenula hookeri*, *Bromus carinatus*, *Carex plantaginea*, and *Poa secunda* subsp. *Secunda* each had sample sizes of five or less (Table 3-1).

The two processes that are likely most important at shaping selection on pollen size in wind-pollinated species are selection during pollen transport by the wind and selection imposed by post-pollination processes like pollen germination and pollen tube growth. As described in Section 1.3, wind pollination imposes balancing selection on pollen size during pollen transport, where lighter, smaller pollen can be removed from stigmas more easily and transported further but larger pollen is more likely to successfully impact a stigma (Whitehead 1969). However, after pollen lands on a stigma, to successfully fertilize an ovule it must germinate a pollen tube that can grow down the style and reach an unfertilized ovule. This latter process is thought to be the main source of selection on pollen size in animal-pollinated plants, rather than selection imposed by pollinators during pollen transport (Harder 1998). If multiple grains land on a stigma, pollen competition occurs as grains compete to fertilize limited ovules (Stephenson and Bertin 1983, Delph and Havens 1998). Pollen size is associated with competitive ability during pollen competition, with larger pollen having more resources available for faster germination and pollen tube growth (Baker and Baker 1979). Larger pollen outcompetes smaller grains during pollen competition in *Ipomoea purpurea* plants with genetically determined differences in pollen size, suggesting that pollen size might be a genetic-based indicator of pollen vigour (McCallum and Chang 2016). Pollen competition might be especially important in wind-pollinated species for several reasons. First, almost all wind-pollinated species have just one ovule per flower, which facilitates pollen competition even under relatively small pollen loads. Additionally, flowering and pollen release tends to be highly synchronous in wind-pollinated plants (Dowding 1987), finishing in just 2-3h for some grass species (Heslop-Harrison 1979), which could allow

multiple grains to arrive and germinate on a stigma at once. Further, pollen size might be especially important in providing resources for growth and determining competitive ability. While pollen tubes in some species rely on stelar resources to fuel their growth (e.g. lilies), grasses often rely on resources contained within the pollen grain itself, which should strengthen the association between pollen size and competitive ability (Heslop-Harrison 1979). Selection on pollen size may therefore be especially strong in wind-pollinated species, both during pollen transport and post-pollination, from pollen competition.

If selection on a trait is strong, we might expect relatively little variation in it. Correspondingly, pollen size was four- to forty-times less variable than pollen production across all 31 species, based on coefficients of variation (Table 3-1), a significant difference. This pattern of pollen diameter being far less variable than pollen number appears to be consistent across multiple species. For example, in a survey of 21 legume species, coefficients of variation for pollen number varied four to ten times more than those for pollen diameter within species, suggesting that pollen size is likely under strong selection compared to pollen number (Vonhof and Harder 1995). Similar results were found when comparing CVs for pollen number per flower and pollen volume across 40 *Pedicularis* species (Yang and Guo 2004). Compared to these surveys of animal-pollinated species, the average CV in pollen size was smaller for the sample of wind-pollinated species from diverse families (average CV=3.7%) than the average CV for 21 legume species (average CV=3.9%, Table 2 Vonhof and Harder 1995) or 40 *Pedicularis* species (average CV=10.6%, Yang and Guo 2003). The relatively small variability in pollen size suggests that pollen size may be both more developmentally constrained under reproductive resource variability, and that pollen size may be under stronger stabilizing selection than pollen number (Vonhof and Harder 1995, Sarkissian and Harder 2001, Yang and Guo 2004).

The evolution of pollen size may also be influenced by a species' sex system. Pollen dispersal is likely more important in dioecious species than monoecious or hermaphroditic species, given that they cannot self-pollinate and not all neighbours are potential mates (Cruden 2000). This may favour the evolution of smaller, further-dispersing pollen in dioecious species, since smaller pollen has a lower settling velocity, which may allow grains to travel further before settling out of the airstream. Analysis of pollen size using a mixed effects model revealed that pollen size in dioecious species was indeed significantly smaller pollen than that of hermaphroditic species (Figure 3-3). In monoecious species, pollen diameter was not significantly different from either dioecious or hermaphroditic species (Figure 3-3). Similar connections between sex system and pollen size have been found in *Plantago lanceolata*. In a population with both hermaphroditic and female individuals, female variants of *P. lanceolata* received smaller pollen grains than their hermaphroditic counterparts (Primack 1978). Smaller pollen size was also associated with the density of a plant's local mating neighbourhood, with pollen size also decreasing with increasing distance from a female to its closest mating partners (Primack 1978). This suggests that smaller pollen has a dispersal advantage over larger pollen, which will be advantageous when plants are isolated or cannot self-pollinate.

However, when phylogenetic relatedness between species was accounted for using a PGLS model, there was no significant effect of sex system on pollen size, suggesting that pollen size may be more related to a species' phylogeny than its sex system. A close relationship between phylogeny and pollen size may be expected given that pollen size has a large impact on pollen release, transport, and capture, all of which will be influenced by the size and structure of a plant's inflorescences and its local wind environment. For example, short-statured understory sedges likely experience lower windspeeds and less frequent winds than tall grasses that populate

wide-open fields. Additionally, species where pollen release is facilitated by direct contact with wind gusts to anthers may experience different selection pressures on pollen size than plants where pollen removal is facilitated mainly by stamen resonance.

4.2 Evolution of ovule number

The association between wind pollination and low ovule number was thought to result from a low probability of pollen receipt, making it wasteful to package multiple ovules per flower if stigmas are unlikely to receive multiple grains per flower (Dowding 1987). However, pollen loads are not necessarily low in wind-pollinated plants. For the species included in this analysis, average pollen capture exceeded ovule number for all 19 species, all of which have one ovule per carpel but *Plantago lanceolata*, which has two. For over half of the species, mean stigmatic pollen loads exceeded 10 grains per ovule. While some species had distributions of pollen capture that peaked around 0 or 1 (e.g., *Carex stipata*, *Rumex acetosella*, *Thalictrum dioicum*), many had peaks close to 10 (*Carex communis*, *Carex hirtifolia*, *Carex pedunculata*, *Scirpus microcarpus*) and some had peaks close to 100 (*Elymus innovatus*, *Elymus repens*, *Plantago lanceolata*, *Plantago major*). This suggests that the probability of pollen receipt in wind-pollinated plants is not necessarily low and therefore may not be responsible for their low ovule numbers. In this section, I explore several factors that may shape pollen receipt, including broader influences like sex system and mating system as well as more local influences from a plant's pollination environment, such as its height, local mate density, stigma length, and the date stigmas were sampled. Of these influences, sex system, sampling date, and stigma length were especially important in determining stigmatic pollen load.

The separation of sex functions in a plant may influence pollen capture by affecting the likelihood of self- and outcrossed pollen transfer, with increasing separation of the sexes likely

resulting in a lower probability of pollen receipt. Overall, hermaphroditic species received significantly more pollen than monoecious or dioecious species (Figure 3-5). Higher pollen loads in hermaphroditic species compared to dioecious or monoecious species could be explained by several factors. First, in a hermaphroditic population all individuals in a population are potential mating partners, which could allow for a greater local density of mates compared to a dioecious population. Additionally, since hermaphroditic flowers share both male and female functions, much of the pollen on stigmas could be from self-pollination. Therefore, not all pollen found on these stigmas may be viable, if species are self-incompatible, as is the case in many hermaphroditic species in this analysis, including *Agrostis stolonifera* (Davies 1953), *Bromus inermis* (Adams 1953), *Elymus repens* (Szczepaniak et al. 2009), *Leymus innovatus* (Dewey 1983), and *Plantago lanceolata* (Ross 1973). In these species, pollen capture may be an overestimate of the number of viable pollen grains on a stigma. Therefore, even though pollen loads may be lower in dioecious or monoecious species, it is possible the pollen on these stigmas is better quality and that the number of grains that can contribute to seed set in each sex system is more similar than it appears. However, pollen loads are only a proxy for the number of pollen grains that can facilitate ovule fertilization. A more accurate measure of pollination success for future analyses would be to quantify the number of pollen tubes in each style that reach the ovary.

Pollen receipt was closely tied to a plant's local pollination environment in several contexts, including timing, plant height, the density of local mates, and the length of a flower's stigmas. The most prevalent influence on pollen capture was the date that stigmas were sampled. Timing is likely highly important for pollination success in wind-pollinated plants. Pollen release in wind-pollinated plants is dependent on appropriate meteorological conditions to facilitate

pollen transport. Flowering in grass populations tends to occur in short bursts at specific times of day, with pollen release more likely in favourable weather conditions (Hyde and Williams 1945). The pollination process can be highly rapid in grasses, with both short-lived stigmas and pollen grains. In *Avena* and *Dactylis*, stigmas are receptive for as little as an hour (Heslop-Harrison 2000). Short windows of synchronous flowering may maximize the chances of successful pollen transfer and receipt, while minimizing the probability of receiving heterospecific pollen.

Temporal separation of male and female function in species may also influence patterns of pollen capture over time. Many wind-pollinated species are protogynous, potentially to reduce the likelihood of self-pollination (Sargent and Otto 2004). In the protogynous species *C. communis*, *C. pedunculata*, *C. plantaginea*, *C. stipata*, and *P. lanceolata*, pollen capture tended to increase over time (Figure B-2, Table 3-4). Since stigmas are receptive before anthers dehisce in protogynous species, stigmatic pollen loads may increase with time as anthers open.

Given that pollen dispersal in wind-pollinated plants tends to be highly local, the density of pollen-producing neighbours surrounding a plant should impact its pollen receipt. Plants with the shortest distance to their five-nearest pollen producing neighbours had higher pollen loads in *C. stipata* and *Rumex acetosella* (Table 3-4). Local mate density was also lowest in these two species (Table A-4), which might suggest that density begins to impact pollen capture only when it is especially low. A similar pattern has been observed in the dioecious wind-pollinated species *Thalictrum fendleria* and *T. dioicum*, where seed set decreased with increased distance from pollen donors in low-density but not high-density populations (Steven and Waller 2007). Therefore, the effects of density on pollen receipt are likely case-specific, important when individuals are isolated, as may be the case for understory grasses, sedges or herbs where

individuals may be far from their nearest neighbour, but unlikely in grassland species, for example, that tend to exist as large monocultures.

While plant height was also expected to be important in determining pollen capture, height had little effect on pollen loads for the species sampled. In only one species, *C. stipata*, taller plants received more pollen (Table 3-4). This contradicts my expectation that shorter plants would have higher pollen loads than taller plants because they are more likely to exist in other plants' pollen shadows. Additionally, *C. stipata* was also one of the few species for which density also affected pollen loads, where plants with closer neighbours tended to receive more pollen. While many *Carex* species are highly selfing (Friedman and Barrett 2009a), the strong influence of height and density on pollen capture in *C. stipata* suggest outcrossing may be important in this species.

The aerodynamics of pollen capture in wind-pollinated plants suggests that stigma size should be especially important in determining pollen loads. The relationship between stigma size and pollen capture may follow an S-shaped curve, where increasing stigma size increases pollen capture until increasingly larger boundary layers begin to decrease pollen capture by deflecting passing grains (Paw U and Hotton 1989, Friedman and Barrett 2011). Correspondingly, longer stigmas received more pollen in 9 of 13 species (Figure 3-4, Figure B-5). In the species where stigma length did not affect pollen capture, self-pollination may be important.

The capacity for self-pollination may limit how local factors like timing, height, density, and stigma length affect pollen capture. For example, *Carex* species tend to be highly selfing (Friedman and Barrett 2009a) and both *Schizachne purpurascens* and *Scirpus microcarpus* exhibit the low pollen production but relatively high pollen receipt characteristic of a selfing syndrome (Table 3-1). The four species where stigma length did not affect pollen capture were

C. pedunculata, *C. plantaginea*, *S. purpurascens*, and *S. microcarpus*. Height and density also failed to affect pollen capture in these species, along with *C. album*, which is primarily self-fertilizing (Yerka et al. 2012).

Rather than low ovule number being a consequence of low pollen receipt, it may instead be part of a pollen capture strategy wind-pollinated plants can exploit because their floral costs are relatively low. The relationship between ovule number and floral investment under variable pollination has been well-studied with theoretical models. Burd's (1995) model for optimal ovule packaging predicted that when pollination is stochastic, increasingly unpredictable pollination should select for increasingly high ovule number per flower, so that plants can take advantage of occasional high pollen loads – except when flowers are relatively cheap compared to ovules. In that case, plants may benefit from producing more, cheaper flowers. This may be the case in wind-pollinated plants, where flowers tend to be relatively inexpensive, with no scents or nectar and reduced perianths. Instead, floral costs in wind-pollinated plants may be related to their investment in pollen capture. Larger stigmas will have greater surface areas to catch pollen, though the benefits of increasingly large stigma size may be limited as larger stigmas will have correspondingly larger boundary layers that will tend to deflect pollen (Paw U and Hotton 1989). Indeed, stigma size was positively and significantly related to pollen capture in 9 of 13 wind-pollinated species. If wind-pollinated species experience a floral resource trade-off, where flowers with larger stigmas are more expensive but can capture more pollen per stigma, and pollination or fertilization success is stochastic, the benefits from making larger flowers that capture more pollen are reduced compared to plants that produce more, cheaper flowers (Friedman and Barrett 2011). Therefore, producing flowers with few ovules may be a strategy to

maximize fitness when pollination is unpredictable by using many cheap flowers to sample more of the airstream.

Alternatively, low ovule numbers may also be advantageous in wind-pollinated plants if they allow for increased pollen competition. Synchronous flowering in wind-pollinated populations (Dowding 1987) may lead to large amounts of pollen arriving on stigmas in quick succession, allowing for brief intense periods of pollen competition. Additionally, since wind-borne pollen is often transported as single grains rather than clumps, this might mean that pollen competing on a stigma arrives from multiple paternal donors, which should intensify competition. Intensifying pollen competition by reducing ovule number below typical pollen loads may lead to more vigorous progeny, if pollen competitive ability is a signal of good quality pollen (Mulcahy and Mulcahy 1975). The importance of pollen competitive ability in wind-pollinated species may be evident in their many adaptations toward fast-germinating pollen. Many families with wind-pollinated members, such as the Poaceae and the Asteraceae, have trinucleate pollen (Brewbaker 1967), which allows for rapid pollen germination, though at the cost of short pollen viability. In the sedges (Cyperaceae), plants produce specialized pseudomonad pollen, where pollen grains initially enclose four microspores but three abort during development and become absorbed into the final pollen grain, resulting in high-investment pollen grains that are both fast-germinating and relatively long-lived (Rocha et al. 2018). These pollen adaptations suggest that pollen competitive ability likely has important consequences for wind-pollinated species. As such, low ovule number in wind-pollinated plants may also function as a mechanism to increase fitness by selecting for high-quality pollen that will produce high quality offspring.

4.3 Influence of phylogeny

Phylogeny had a significant effect on pollen size but not pollen production or capture. Pollen size in wind-pollinated plants is likely affected by both the aerodynamics of wind pollination as well as post-pollination processes like pollen germination, pollen tube growth, and pollen competition. Pollen capture tends to be highly variable, both within and across individuals within a species, and is therefore less likely to be influenced by phylogeny. Compared to pollen production, pollen size may be more strongly genetically determined, as suggested by the significantly lower variability in pollen size than production. Since pollen release and capture depends on pollen aerodynamics, the structure of inflorescences or flowers interacting with the wind likely shape optimal pollen sizes in a group if members in closely related groups tend to have share similar floral or inflorescence structures. For example, in plants that rely on wind gusts to remove pollen, larger pollen and less dense pollen grains will be more easily removed from stigmas lift or drag generated from wind gusts (Timerman and Barrett 2021). However, in species where mechanical motion from shaking anthers is more important for pollen release, this may be less important. Additionally, the size of flowers or inflorescences that capture pollen will also influence optimal pollen size, where plants with larger structures tend to have larger pollen grains that can more easily penetrate their larger boundary layers (Friedman and Harder 2005). Given the close relationship between floral structures and pollen size, phylogenetic signal in pollen size is unsurprising.

4.4 Summary

Despite long being considered inefficient, wind pollination appears to be no less efficient than animal pollination in terms of pollen loss during transport. Pollen transfer efficiencies were similar to those observed in animal-pollinated species, suggesting extensive pollen loss during

wind pollination may not be the cause of high pollen production in wind-pollinated species. Instead, sex system, mating system, and correlated evolution with pollen size may be more important determinants of pollen production. Compared to pollen production, pollen diameter was significantly less variable, suggesting that it may be under stronger balancing selection or genetic constraint than pollen production. Pollen production tended to be higher in hermaphroditic species than monoecious species, however, this may be related to outcrossing rate rather than sex system. A negative relationship between pollen production per anther and pollen volume was observed in six species, while a positive relationship was observed in one. Phylogeny significantly influenced pollen size, but not production, potentially because of strong constraints on pollen size or because of aerodynamic considerations associated with a species' inflorescence architecture. In terms of pollen capture, wind-pollinated stigmas received greater pollen loads than their ovule numbers. Pollen loads were strongly influenced by stigma length and plants' local pollination neighbourhoods, especially the timing of sampling. Increased distance from pollen donors reduced pollen capture only in species with the lowest local mate densities. Plant height had little effect on pollen load. In species where neighbourhood effects had little effect on pollen loads, self-pollination may have obscured patterns. Pollen capture was greater in hermaphroditic species than in dioecious or monoecious species, but much of this pollen may be self-pollen and may not be as high quality as that on dioecious or monoecious stigmas. My results suggest that neither the probability of successful pollen transport nor the probability of pollen receipt is as low as was previously thought in wind-pollinated plants, as would be expected in a widespread pollination strategy.

References

- Ackerly, D. D., and M. Jasiński. 1990. Size-dependent variation of gender in high density stands of the monoecious annual, *Ambrosia artemisiifolia* (Asteraceae). *Oecologia* 82:474–477.
- Ackerman, J. D. 2000. Abiotic pollen and pollination: ecological, functional, and evolutionary perspectives. Pages 167–185 in A. Dafni, M. Hesse, and E. Pacini, editors. *Pollen and Pollination*. Springer, Vienna.
- Adams, M. W. 1953. Cross- and self-incompatibility in relation to seed-setting in *Bromus inermis*. *Botanical Gazette* 115:95–105.
- Aljiboury, A. A., and J. Friedman. 2022. Mating and fitness consequences of variation in male allocation in a wind-pollinated plant. *Evolution* 76:1762–1775.
- Baker, H. G., and I. Baker. 1979. Starch in Angiosperm Pollen Grains and Its Evolutionary Significance. *American Journal of Botany* 66:591–600.
- Bartoń, K. 2023. MuMIn: Multi-Model Inference.
- Bateman, A. 1947. Contamination in seed crops. III. Relation with isolation distance. *Heredity* 1:303–336.
- Bates, D., M. Mächler, B. Bolker, and S. Walker. 2015. Fitting Linear Mixed-Effects Models Using lme4. *Journal of Statistical Software* 67:1–48.
- Brewbaker, J. L. 1967. The distribution and phylogenetic significance of binucleate and trinucleate pollen grains in the Angiosperms. *American Journal of Botany* 54:1069–1083.
- Burd, M. 1995. Ovule packaging in stochastic pollination and fertilization environments. *Evolution* 49:100–109.
- Burd, M., and T. F. H. Allen. 1988. Sexual allocation strategy in wind-pollinated plants. *Evolution* 42:403–407.
- Casper, B. B., and R. A. Niesenbaum. 1993. Pollen versus resource limitation of seed production: A reconsideration. *Current Science* 65:210–214.

- Charlesworth, D., and B. Charlesworth. 1981. Allocation of resources to male and female functions in hermaphrodites. *Biological Journal of the Linnean Society* 15:57–74.
- Charnov, E. L. 1979. Simultaneous hermaphroditism and sexual selection. *Proceedings of the National Academy of Sciences* 76:2480–2484.
- Charnov, E. L. 1982. *The theory of sex allocation*. Princeton University Press.
- Cruden, R. W. 1977. Pollen-ovule ratios: A conservative indicator of breeding systems in flowering plants. *Evolution* 31:32–46.
- Cruden, R. W. 2000. Pollen grains: Why so many? *Plant Systematics and Evolution* 222:143–165.
- Davies, W. E. 1953. The breeding affinities of some British species of *Agrostis*.
- Delph, L., and K. Havens. 1998. Pollen competition in flowering plants. Pages 149–173 in T. Birkhead and A. Møller, editors. *Sperm competition and sexual selection*. Academic Press, San Diego, CA, USA.
- Dewey, D. R. 1983. Historical and current taxonomic perspectives of *Agropyron*, *Elymus*, and related genera. *Crop Science* 23:637–642.
- Dowding, P. 1987. Wind pollination mechanisms and aerobiology. Pages 421–437 in G. H. Bourne, K. W. Jeon, and M. Friedlander, editors. *International Review of Cytology*. Academic Press.
- Eppley, S. M., and J. R. Pannell. 2007. Density-dependent self-fertilization and male versus hermaphrodite siring success in an androdioecious plant. *Evolution* 61:2349–2359.
- Faegri, K., and L. Van der Pijl. 1979. Chapter 6 - Abiotic pollination. Pages 34–41 *Principles of Pollination Ecology (Third Edition)*. Pergamon, Amsterdam.
- Fox, J., and S. Weisberg. 2019. *An R Companion to Applied Regression*. Third. Sage, Thousand Oaks CA.
- Friedman, J., and S. C. H. Barrett. 2008. A phylogenetic analysis of the evolution of wind pollination in the Angiosperms. *International Journal of Plant Sciences* 169:49–58.

- Friedman, J., and S. C. H. Barrett. 2009a. The consequences of monoecy and protogyny for mating in wind-pollinated *Carex*. *New Phytologist* 181:489–497.
- Friedman, J., and S. C. H. Barrett. 2009b. Wind of change: New insights on the ecology and evolution of pollination and mating in wind-pollinated plants. *Annals of Botany* 103:1515–1527.
- Friedman, J., and S. C. H. Barrett. 2011. The evolution of ovule number and flower size in wind-pollinated plants. *The American Naturalist* 177:246–257.
- Friedman, J., and L. D. Harder. 2005. Functional associations of floret and inflorescence traits among grass species. *American Journal of Botany* 92:1862–1870.
- Gleaves, J. T. 1973. Gene flow mediated by wind-borne pollen. *Heredity* 31:355–366.
- Harder, L. D. 1998. Pollen-size comparisons among animal-pollinated angiosperms with different pollination characteristics. *Biological Journal of the Linnean Society* 64:513–525.
- Harder, L. D. 2000. Pollen dispersal and the floral diversity of monocotyledons. Pages 243–257 in K. L. Wilson and D. A. Morrison, editors. *Monocots: systematics and evolution*. CSIRO, Melbourne.
- Harder, L. D., and S. D. Johnson. 2023. Beyond P:O ratios: evolutionary consequences of pollinator dependence and pollination efficiency for pollen and ovule production in angiosperms. *American Journal of Botany* 110:e16177.
- Harder, L. D., and P. Prusinkiewicz. 2013. The interplay between inflorescence development and function as the crucible of architectural diversity. *Annals of Botany* 112:1477–1493.
- Harder, L. D., and J. D. Thomson. 1989. Evolutionary options for maximizing pollen dispersal of animal-pollinated plants. *The American Naturalist* 133:323–344.
- Heath, D. J. 1977. Simultaneous hermaphroditism; cost and benefit. *Journal of Theoretical Biology* 64:363–373.
- Henderson, L. B. 1926. Floral anatomy of several species of *Plantago*. *American Journal of Botany* 13:397–405.

- Heslop-Harrison, J. 1979. Pollen-stigma interaction in grasses: a brief review. *New Zealand Journal of Botany* 17:537–546.
- Heslop-Harrison, Y. 2000. Control gates and micro-ecology: The pollen-stigma interaction in perspective. *Annals of Botany* 85:5–13.
- Hesse, E., and J. R. Pannell. 2011a. Density-dependent pollen limitation and reproductive assurance in a wind-pollinated herb with contrasting sexual systems. *Journal of Ecology* 99:1531–1539.
- Hesse, E., and J. R. Pannell. 2011b. Sexual dimorphism in androdioecious *Mercurialis annua*, a wind-pollinated herb. *International Journal of Plant Sciences* 172:49–59.
- Honig, M. A., H. P. Linder, and W. J. Bond. 1992. Efficacy of wind pollination: pollen load size and natural microgametophyte populations in wind-pollinated *Staberoha banksii* (Restionaceae). *American Journal of Botany* 79:443–448.
- Hu, S., D. L. Dilcher, D. M. Jarzen, and D. W. Taylor. 2008. Early steps of angiosperm–pollinator coevolution. *Proceedings of the National Academy of Sciences* 105:240–245.
- Hyde, H. A., and D. A. Williams. 1945. Studies in atmospheric pollen. II. Diurnal variation in the incidence of grass pollen. *The New Phytologist* 44:83–94.
- Jin, Y., and H. Qian. 2022. V.PhyloMaker2: An updated and enlarged R package that can generate very large phylogenies for vascular plants. *Plant Diversity* 44:335–339.
- Klinkhamer, P. G. L., and T. J. de Jong. 1997. Size-dependent allocation to male and female reproduction. Pages 211–229 in F. A. Bazzaz and J. Grace, editors. *Plant Resource Allocation*. Elsevier.
- Klinkhamer, P. G. L., T. J. de Jong, and H. Metz. 1997. Sex and size in cosexual plants. *Trends in Ecology & Evolution* 12:260–265.
- Knight, T. M., J. A. Steets, J. C. Vamosi, S. J. Mazer, M. Burd, D. R. Campbell, M. R. Dudash, M. O. Johnston, R. J. Mitchell, and T.-L. Ashman. 2005. Pollen limitation of plant reproduction: pattern and process. *Annual Review of Ecology, Evolution, and Systematics* 36:467–497.
- Lenth, R. V. 2023. emmeans: Estimated marginal means, aka least-squares means.

- Levin, D. A., and H. W. Kerster. 1974. Gene flow in seed plants. *Evolutionary Biology*: Volume 7:139–220.
- Linder, H. P. 1998. Morphology and the evolution of wind pollination. Pages 123–135 *Reproductive biology in systematics, conservation and economic botany*. Kew: Royal Botanic Gardens.
- Lundholm, J. T., and L. W. Aarssen. 1994. Neighbour effects on gender variation in *Ambrosia artemisiifolia*. *Canadian Journal of Botany* 72:794–800.
- Mazer, S. J., and U.-M. Hultgård. 1993. Variation and covariation among floral traits within and among four species of Northern European *Primula* (Primulaceae). *American Journal of Botany* 80:474–485.
- McCallum, B., and S.-M. Chang. 2016. Pollen competition in style: Effects of pollen size on siring success in the hermaphroditic common morning glory, *Ipomoea purpurea*. *American Journal of Botany* 103:460–470.
- McKone, M. J. 1987. Sex allocation and outcrossing rate: A test of theoretical predictions using bromegrasses (*Bromus*). *Evolution; International Journal of Organic Evolution* 41:591–598.
- McKone, M. J., and D. W. Tonkyn. 1986. Intrapopulation gender variation in common ragweed (Asteraceae: *Ambrosia artemisiifolia* L.), a monoecious, annual herb. *Oecologia* 70:63–67.
- Meeuse, B. J. D. 1961. *The Story of Pollination*. Ronald Press, New York, NY, USA.
- Mengli, Z., H. Bing, and W. D. Willms. 2008. Detection of genetic diversity in rough fescue (*Festuca campestris* Rydb) populations of southern Alberta and British Columbia, Canada, using RAPD markers. *Canadian Journal of Plant Science* 88:307–312.
- Michalski, S. G., and W. Durka. 2009. Pollination mode and life form strongly affect the relation between mating system and pollen to ovule ratios. *New Phytologist* 183:470–479.
- Michalski, S. G., and W. Durka. 2010. Pollen and ovule production in wind-pollinated species with special reference to *Juncus*. *Plant Systematics and Evolution* 286:191–197.

- Milatović, D., D. Nikolić, S. Janković, D. Janković, and J. Stanković. 2020. Morphological characteristics of male reproductive organs in some walnut (*Juglans regia* L.) genotypes. *Scientia Horticulturae* 272:109587.
- Mulcahy, D. L., and G. B. Mulcahy. 1975. The influence of gametophytic competition on sporophytic quality in *Dianthus chinensis*. *Theoretical and Applied Genetics* 46:277–280.
- Muller, J. 1979. Form and function in angiosperm pollen. *Annals of the Missouri Botanical Garden* 66:593–632.
- Niklas, K. J. 1982. Simulated and empiric wind pollination patterns of conifer ovulate cones. *Proceedings of the National Academy of Sciences* 79:510–514.
- Niklas, K. J. 1984. The motion of windborne pollen grains around conifer ovulate cones: Implications of wind pollination. *American Journal of Botany* 71:356–374.
- Niklas, K. J. 1985. The aerodynamics of wind pollination. *The Botanical Review* 51:328–386.
- Niklas, K. J. 1992. *Plant Biomechanics: An Engineering Approach to Plant Form and Function*. University of Chicago Press, Chicago, IL, USA.
- Niklas, K. J., and S. L. Buchmann. 1987. The aerodynamics of pollen capture in two sympatric *Ephedra* species. *Evolution* 41:104–123.
- Niklas, K. J., and K. T. Paw U. 1982. Pollination and airflow patterns around conifer ovulate cones. *Science* 217:442–444.
- Okubo, A., and S. A. Levin. 1989. A theoretical framework for data analysis of wind dispersal of seeds and pollen. *Ecology* 70:329–338.
- Ollerton, J., R. Winfree, and S. Tarrant. 2011. How many flowering plants are pollinated by animals? *Oikos* 120:321–326.
- Orme, D., R. Freckleton, G. Thomas, T. Petzoldt, S. Fritz, N. Isaac, and W. Pearse. 2018. *caper: Comparative analyses of phylogenetics and evolution in R*.

- Paquin, V., and L. W. Aarssen. 2004. Allometric gender allocation in *Ambrosia artemisiifolia* (Asteraceae) has adaptive plasticity. *American Journal of Botany* 91:430–438.
- Parachnowitsch, A. L., and E. Elle. 2004. Variation in sex allocation and male–female trade-offs in six populations of *Collinsia parviflora* (Scrophulariaceae s.l.). *American Journal of Botany* 91:1200–1207.
- Paw U, K. T. P., and C. Hotton. 1989. Optimum pollen and female receptor size for anemophily. *American Journal of Botany* 76:445–453.
- Primack, R. B. 1978. Evolutionary aspects of wind pollination in the genus *Plantago* (Plantaginaceae). *New Phytologist* 81:449–458.
- Proctor, M., and P. Yeo. 1973. *The Pollination of Flowers*. Collins, London, UK.
- Proctor, M., P. F. Yeo, P. Yeo, and A. Lack. 1996. *The Natural History of Pollination*. Timber Press, Portland, Oregon, USA.
- Qian, H., and Y. Jin. 2016. An updated megaphylogeny of plants, a tool for generating plant phylogenies and an analysis of phylogenetic community structure. *Journal of Plant Ecology* 9:233–239.
- R Core Team. 2023. *R: A language and environment for statistical computing*. R Foundation for Statistical Computing, Vienna, Austria.
- Renner, S. S. 2014. The relative and absolute frequencies of angiosperm sexual systems: Dioecy, monoecy, gynodioecy, and an updated online database. *American Journal of Botany* 101:1588–1596.
- Rocha, D., A. Vanzela, and J. Mariath. 2018. Comparative study of microgametogenesis in members of Cyperaceae and Juncaceae: A shift from permanent pollen tetrads to pseudomonads. *Botanical Journal of the Linnean Society* 188:59.
- Rognli, O. A., N.-O. Nilsson, and M. Nurminiemi. 2000. Effects of distance and pollen competition on gene flow in the wind-pollinated grass *Festuca pratensis* Huds. *Heredity* 85:550–560.
- Ross, M. D. 1973. Inheritance of self-incompatibility in *Plantago lanceolata*. *Heredity* 30:169–176.

- Sargent, R. D., and S. P. Otto. 2004. A phylogenetic analysis of pollination mode and the evolution of dichogamy in angiosperms. *Evolutionary Ecology Research* 6:1183–1199.
- Sarkissian, T. S., and L. D. Harder. 2001. Direct and indirect responses to selection on pollen size in *Brassica rapa* L. *Journal of Evolutionary Biology* 14:456–468.
- Schneider, C. A., W. S. Rasband, and K. W. Eliceiri. 2012. NIH Image to ImageJ: 25 years of image analysis. *Nature Methods* 9:671–675.
- Schoen, D. J., and S. C. Stewart. 1986. Variation in male reproductive investment and male reproductive success in white spruce. *Evolution* 40:1109–1120.
- Schreiber, S. J., J. A. Rosenheim, N. W. Williams, and L. D. Harder. 2015. Evolutionary and ecological consequences of multiscale variation in pollen receipt for seed production. *The American Naturalist* 185:E14-29.
- Scofield, D. G., and S. T. Schultz. 2005. Mitosis, stature and evolution of plant mating systems: low- Φ and high- Φ plants. *Proceedings of the Royal Society B: Biological Sciences* 273:275–282.
- Stanton, M., and H. J. Young. 1994. Selecting for floral character associations in wild radish, *Raphanus sativus* L. *Journal of Evolutionary Biology* 7:271–285.
- Stehlik, I., J. Friedman, and S. C. H. Barrett. 2008. Environmental influence on primary sex ratio in a dioecious plant. *Proceedings of the National Academy of Sciences* 105:10847–10852.
- Stephenson, A., and R. Bertin. 1983. Male competition, female choice, and sexual selection in plants. Pages 109–151 in L. Real, editor. *Pollination Biology*. Academic Press, New York, NY, USA.
- Steven, J. C., and D. M. Waller. 2007. Isolation affects reproductive success in low-density but not high-density populations of two wind-pollinated *Thalictrum* species. *Plant Ecology* 190:131–141.
- Szczepaniak, M., W. Bieniek, P. Boroń, M. Szklarczyk, and M. Mizianty. 2009. A contribution to characterisation of genetic variation in some natural Polish populations of *Elymus repens* (L.) Gould and *Elymus hispidus* (Opiz) Melderis (Poaceae) as revealed by RAPD markers. *Plant Biology* 11:766–773.

- Timerman, D., and S. C. H. Barrett. 2019. Comparative analysis of pollen release biomechanics in *Thalictrum*: implications for evolutionary transitions between animal and wind pollination. *New Phytologist* 224:1121–1132.
- Timerman, D., and S. C. H. Barrett. 2021. The biomechanics of pollen release: new perspectives on the evolution of wind pollination in angiosperms. *Biological Reviews* 96:2146–2163.
- Timerman, D., D. F. Greene, J. Urzay, and J. D. Ackerman. 2014. Turbulence-induced resonance vibrations cause pollen release in wind-pollinated *Plantago lanceolata* L. (Plantaginaceae). *Journal of The Royal Society Interface* 11:20140866.
- Tonsor, S. J. 1985. Leptokurtic pollen-flow, non-leptokurtic gene-flow in a wind-pollinated herb, *Plantago lanceolata* L. *Oecologia* 67:442–446.
- Traveset, A. 1992. Sex expression in a natural population of the monoecious annual, *Ambrosia artemisiifolia* (Asteraceae). *The American Midland Naturalist* 127:309–315.
- Urzay, J., S. G. Llewellyn Smith, E. Thompson, and B. J. Glover. 2009. Wind gusts and plant aeroelasticity effects on the aerodynamics of pollen shedding: A hypothetical turbulence-initiated wind-pollination mechanism. *Journal of Theoretical Biology* 259:785–792.
- Vonhof, M. J., and L. D. Harder. 1995. Size-number trade-offs and pollen production by Papilionaceous legumes. *American Journal of Botany* 82:230–238.
- Welsford, M. R., N. Hobbhahn, J. J. Midgley, and S. D. Johnson. 2016. Floral trait evolution associated with shifts between insect and wind pollination in the dioecious genus *Leucadendron* (Proteaceae). *Evolution* 70:126–139.
- Whitehead, D. R. 1969. Wind pollination in the angiosperms: Evolutionary and environmental considerations. *Evolution* 23:28–35.
- Wickham, H. 2016. *ggplot2: Elegant graphics for data analysis*. Springer-Verlag New York.
- Wilke, C. O. 2022. *ggridges: Ridgeline plots in “ggplot2.”*

- Wodehouse, R. P. 1935. Pollen grains. Their structure, identification and significance in science and medicine. McGraw-Hill, New York, NY, USA.
- Yang, C.-F., and Y.-H. Guo. 2004. Pollen size-number trade-off and pollen-pistil relationships in *Pedicularis* (Orobanchaceae). *Plant Systematics and Evolution* 247:177–185.
- Yerka, M. K., N. de Leon, and D. E. Stoltenberg. 2012. Pollen-mediated gene flow in common lambsquarters (*Chenopodium album*). *Weed Science* 60:600–606.

Appendix A

Supplemental Tables

Table A-1. Sampling details and list of all species where pollen production and size were quantified. N is the number of individuals measured per species.

Species	Family	Sex system	Source	N
<i>Agrostis stolonifera</i>	Poaceae	Hermaphroditic	Kananaskis, AB, 2001-2002	4
<i>Amaranthus retroflexus</i>	Amaranthaceae	Monoecious	Kingston, ON, 2021	16
<i>Ambrosia artemisiifolia</i>	Asteraceae	Monoecious	Kingston, ON, 2021	10
<i>Ambrosia artemisiifolia</i>	Asteraceae	Monoecious	Koffler Scientific Reserve, ON, 2004	21
<i>Avenula hookeri</i>	Poaceae	Hermaphroditic	Kananaskis, AB, 2001-2002	5
<i>Bromus carianatus</i>	Poaceae	Hermaphroditic	Kananaskis, AB, 2001-2002	3
<i>Bromus inermis</i>	Poaceae	Hermaphroditic	Kananaskis, AB, 2001-2002	30
<i>Carex communis</i>	Cyperaceae	Monoecious	Koffler Scientific Reserve, ON, 2004	18
<i>Carex hirtifolia</i>	Cyperaceae	Monoecious	Koffler Scientific Reserve, ON, 2004	18
<i>Carex pedunculata</i>	Cyperaceae	Monoecious	Koffler Scientific Reserve, ON, 2004	19
<i>Carex plantaginea</i>	Cyperaceae	Monoecious	Koffler Scientific Reserve, ON, 2004	4
<i>Carex stipata</i>	Cyperaceae	Monoecious	Koffler Scientific Reserve, ON, 2004	36
<i>Chenopodium album</i>	Amaranthaceae	Hermaphroditic	Kingston, ON, 2021	19
<i>Chenopodium album</i>	Amaranthaceae	Hermaphroditic	Koffler Scientific Reserve, ON, 2004	22
<i>Elymus innovatus</i>	Poaceae	Hermaphroditic	Kananaskis, AB, 2001-2002	35
<i>Elymus repens</i>	Poaceae	Hermaphroditic	Kananaskis, AB, 2001-2002	33
<i>Elymus trachycaulus</i>	Poaceae	Hermaphroditic	Kananaskis, AB, 2001-2002	10
<i>Festuca campestris</i>	Poaceae	Hermaphroditic	Kananaskis, AB, 2001-2002	60
<i>Festuca pratensis</i>	Poaceae	Hermaphroditic	Kananaskis, AB, 2001-2002	14
<i>Festuca rubra</i>	Poaceae	Hermaphroditic	Kananaskis, AB, 2001-2002	8
<i>Hierochloa odorata</i>	Poaceae	Hermaphroditic	Kananaskis, AB, 2001-2002	67
<i>Koeleria cristata</i>	Poaceae	Hermaphroditic	Kananaskis, AB, 2001-2002	25
<i>Phalaris arundinacea</i>	Poaceae	Hermaphroditic	Kananaskis, AB, 2001-2002	7

<i>Phleum pratense</i>	Poaceae	Hermaphroditic	Kananaskis, AB, 2001-2002	30
<i>Plantago lanceolata</i>	Plantaginaceae	Hermaphroditic	Kingston, ON, 2021	28
<i>Plantago lanceolata</i>	Plantaginaceae	Hermaphroditic	Koffler Scientific Reserve, ON, 2004	24
<i>Poa juncifolia</i>	Poaceae	Hermaphroditic	Kananaskis, AB, 2001-2002	6
<i>Poa secunda subsp. secunda</i>	Poaceae	Hermaphroditic	Kananaskis, AB, 2001-2002	3
<i>Rumex acetosella</i>	Polygonaceae	Dioecious	Kingston, ON, 2021	9
<i>Rumex acetosella</i>	Polygonaceae	Dioecious	Koffler Scientific Reserve, ON, 2004	21
<i>Rumex crispus</i>	Polygonaceae	Monoecious	Koffler Scientific Reserve, ON, 2004	20
<i>Schizachne purpurascens</i>	Poaceae	Hermaphroditic	Koffler Scientific Reserve, ON, 2004	12
<i>Scirpus microcarpus</i>	Cyperaceae	Monoecious	Koffler Scientific Reserve, ON, 2004	14
<i>Stipa columbiana</i>	Poaceae	Hermaphroditic	Kananaskis, AB, 2001-2002	10
<i>Thalictrum dioicum</i>	Ranunculaceae	Dioecious	Kingston, ON, 2021	7
<i>Thalictrum dioicum</i>	Ranunculaceae	Dioecious	Koffler Scientific Reserve, ON, 2004	23

Table A-2. Sampling details and list of all species where stigmatic pollen receipt was quantified. N is the number of individuals measured per species.

Species	Family	Sex system	Source	N
<i>Amaranthus retroflexus</i>	Amaranthaceae	Monoecious	Kingston, ON, 2021	30
<i>Ambrosia artemisiifolia</i>	Asteraceae	Monoecious	Kingston, ON, 2021	30
<i>Ambrosia artemisiifolia</i>	Asteraceae	Monoecious	Koffler Scientific Reserve, ON, 2004	30
<i>Bromus inermis</i>	Poaceae	Hermaphroditic	Kananaskis, AB, 2001-2002	67
<i>Carex communis</i>	Cyperaceae	Monoecious	Koffler Scientific Reserve, ON, 2004	22
<i>Carex hirtifolia</i>	Cyperaceae	Monoecious	Koffler Scientific Reserve, ON, 2004	48
<i>Carex pedunculata</i>	Cyperaceae	Monoecious	Koffler Scientific Reserve, ON, 2004	23
<i>Carex plantaginea</i>	Cyperaceae	Monoecious	Koffler Scientific Reserve, ON, 2004	27
<i>Carex stipata</i>	Cyperaceae	Monoecious	Koffler Scientific Reserve, ON, 2004	30
<i>Chenopodium album</i>	Amaranthaceae	Hermaphroditic	Kingston, ON, 2021	30
<i>Chenopodium album</i>	Amaranthaceae	Hermaphroditic	Koffler Scientific Reserve, ON, 2004	30
<i>Dichanthelium implicatum</i>	Poaceae	Hermaphroditic	Kingston, ON, 2021	40
<i>Dichanthelium linearifolium</i>	Poaceae	Hermaphroditic	Kingston, ON, 2021	20
<i>Elymus repens</i>	Poaceae	Hermaphroditic	Kananaskis, AB, 2001-2002	41
<i>Festuca campestris</i>	Poaceae	Hermaphroditic	Kananaskis, AB, 2001-2002	83
<i>Leymus innovatus</i>	Poaceae	Hermaphroditic	Kananaskis, AB, 2001-2002	79
<i>Phleum pratense</i>	Poaceae	Hermaphroditic	Kingston, ON, 2021	22
<i>Phleum pratense</i>	Poaceae	Hermaphroditic	Kananaskis, AB, 2001-2002	69
<i>Plantago lanceolata</i>	Plantaginaceae	Hermaphroditic	Kingston, ON, 2021	43
<i>Plantago lanceolata</i>	Plantaginaceae	Hermaphroditic	Koffler Scientific Reserve, ON, 2004	30
<i>Plantago major</i>	Plantaginaceae	Hermaphroditic	Kingston, ON, 2021	16
<i>Rumex acetosella</i>	Polygonaceae	Dioecious	Kingston, ON, 2021	39
<i>Rumex acetosella</i>	Polygonaceae	Dioecious	Koffler Scientific Reserve, ON, 2004	30
<i>Rumex crispus</i>	Polygonaceae	Monoecious	Koffler Scientific Reserve, ON, 2004	25
<i>Schizachne purpurascens</i>	Poaceae	Hermaphroditic	Koffler Scientific Reserve, ON, 2004	31
<i>Scirpus microcarpus</i>	Cyperaceae	Monoecious	Koffler Scientific Reserve, ON, 2004	30
<i>Setaria viridis</i>	Poaceae	Hermaphroditic	Kingston, ON, 2021	45
<i>Thalictrum dioicum</i>	Ranunculaceae	Dioecious	Kingston, ON, 2021	59
<i>Thalictrum dioicum</i>	Ranunculaceae	Dioecious	Koffler Scientific Reserve, ON, 2004	23

Table A-3. Sampling details and list of all species used to analyze the effects of individual-level factors on stigmatic pollen receipt. Species are ordered first by sex system, then alphabetically. N is the number of individuals measured per species.

Species	Family	Sex system	Source	N
<i>Ambrosia artemisiifolia</i>	Asteraceae	Monoecious	Koffler Scientific Reserve, ON, 2004	30
<i>Carex communis</i>	Cyperaceae	Monoecious	Koffler Scientific Reserve, ON, 2004	22
<i>Carex hirtifolia</i>	Cyperaceae	Monoecious	Koffler Scientific Reserve, ON, 2004	48
<i>Carex pedunculata</i>	Cyperaceae	Monoecious	Koffler Scientific Reserve, ON, 2004	23
<i>Carex plantaginea</i>	Cyperaceae	Monoecious	Koffler Scientific Reserve, ON, 2004	27
<i>Carex stipata</i>	Cyperaceae	Monoecious	Koffler Scientific Reserve, ON, 2004	30
<i>Chenopodium album</i>	Amaranthaceae	Hermaphroditic	Koffler Scientific Reserve, ON, 2004	30
<i>Plantago lanceolata</i>	Plantaginaceae	Hermaphroditic	Koffler Scientific Reserve, ON, 2004	30
<i>Rumex acetosella</i>	Polygonaceae	Dioecious	Koffler Scientific Reserve, ON, 2004	30
<i>Rumex crispus</i>	Polygonaceae	Monoecious	Koffler Scientific Reserve, ON, 2004	25
<i>Schizachne purpurascens</i>	Poaceae	Hermaphroditic	Koffler Scientific Reserve, ON, 2004	31
<i>Scirpus microcarpus</i>	Cyperaceae	Monoecious	Koffler Scientific Reserve, ON, 2004	30
<i>Thalictrum dioicum</i>	Ranunculaceae	Dioecious	Koffler Scientific Reserve, ON, 2004	23

Table A-4. Summary of individual-level factors potentially affecting pollen capture for 13 wind-pollinated species. Plant height is a plant’s maximum height in cm, stigma length is the maximum length of a plant’s stigma in cm, and density is measured as the average distance from a plant to its five-nearest pollen-producing neighbours, in cm.

Species	Plant height (cm)				Stigma length (cm)				Density (cm)			
	Mean	Min	Max	SD	Mean	Min	Max	SD	Mean	Min	Max	SD
<i>Ambrosia artemisiifolia</i>	103.3	55.0	158.0	25.9	1.83	0.60	4.10	0.54	17.0	8.0	26.0	5.3
<i>Carex communis</i>	20.4	14.0	26.0	2.9	3.09	1.70	4.30	0.45	30.6	21.4	60.0	10.6
<i>Carex hirtifolia</i>	20.9	17.0	29.0	2.5	2.35	1.20	3.00	0.33	45.5	18.6	103.8	22.1
<i>Carex pedunculata</i>	15.2	11.0	20.0	2.7	4.46	2.90	5.95	0.60	39.6	27.6	61.0	8.2
<i>Carex plantaginea</i>	21.5	15.5	29.0	3.6	4.05	2.00	6.50	0.90	75.9	25.6	400.0	71.3
<i>Carex stipata</i>	38.2	24.0	48.0	5.8	1.68	0.90	2.70	0.32	185.3	75.0	384.0	76.7
<i>Chenopodium album</i>	104.1	64.0	138.0	17.4	0.46	0.20	0.80	0.11	35.3	14.4	72.2	14.5
<i>Plantago lanceolata</i>	42.1	29.0	55.0	7.3	1.72	0.35	4.40	0.64	64.4	25.2	197.0	39.0
<i>Rumex acetosella</i>	28.2	20.0	48.0	7.2	0.62	0.45	0.90	0.10	331.4	15.6	990.0	291.0
<i>Rumex crispus</i>	102.6	85.0	120.0	8.0	0.94	0.38	1.48	0.18	123.7	27.4	795.0	161.6
<i>Schizachne purpurascens</i>	71.4	61.0	81.0	4.8	2.21	0.70	3.00	0.31	94.6	58.0	166.4	23.3
<i>Scirpus microcarpus</i>	74.8	53.0	93.0	10.5	0.91	0.50	1.10	0.10	50.6	15.8	182.0	39.0
<i>Thalictrum dioicum</i>	28.9	18.0	46.0	6.6	2.80	1.60	4.30	0.54	96.7	38.4	319.6	60.1

Appendix B

Supplemental Figures

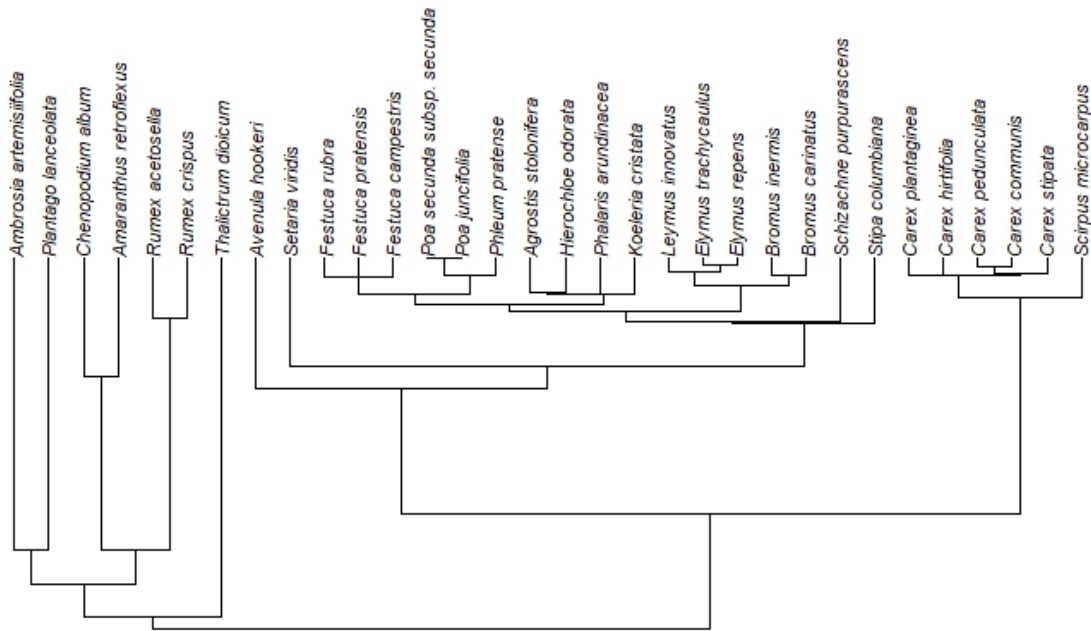


Figure B-1. Phylogeny of 32 wind-pollinated species used in the pollen production and size analysis, generated using the function “*phylomaker*” from the package “*V.PhyloMaker2*” (Jin & Qian 2022) using the seed plant phylogeny *GBOTB.extended.TPL* (Jin & Qian 2022) and the function’s default phylogenetic hypothesis scenario, Scenario 3 (Qian & Jin 2016).

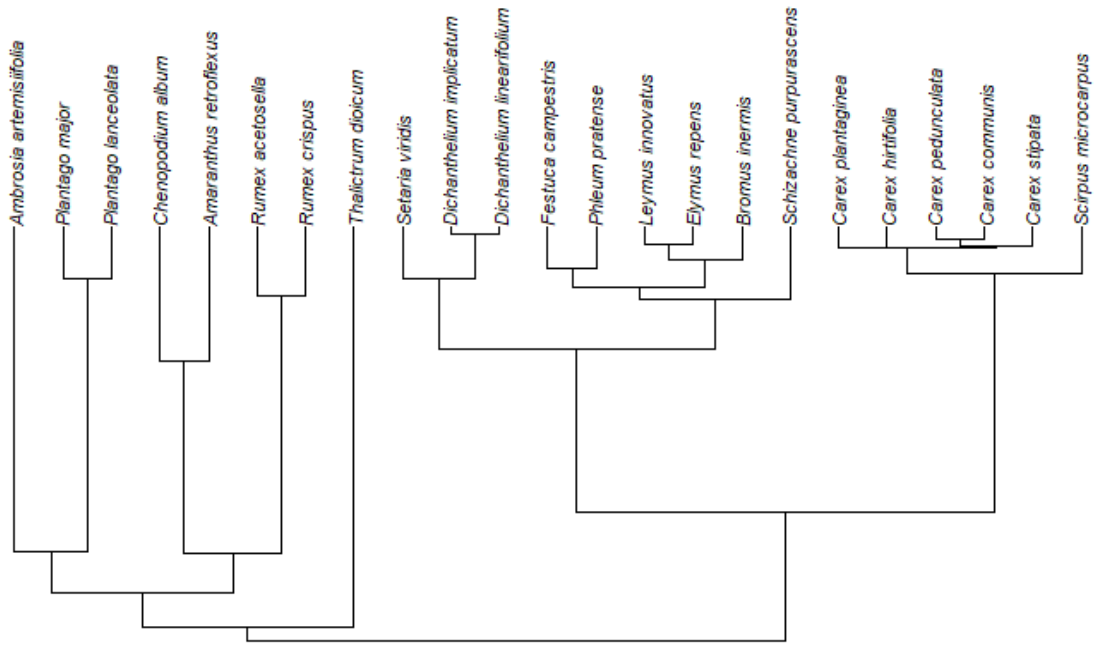


Figure B-2. Phylogeny of 23 wind-pollinated species used in the pollen capture analysis, generated using the function “phylomaker” from the package “V.PhyloMaker2” (Jin & Qian 2022) using the seed plant phylogeny GBOTB.extended.TPL (Jin & Qian 2022) and the function’s default phylogenetic hypothesis scenario, Scenario 3 (Qian & Jin 2016).

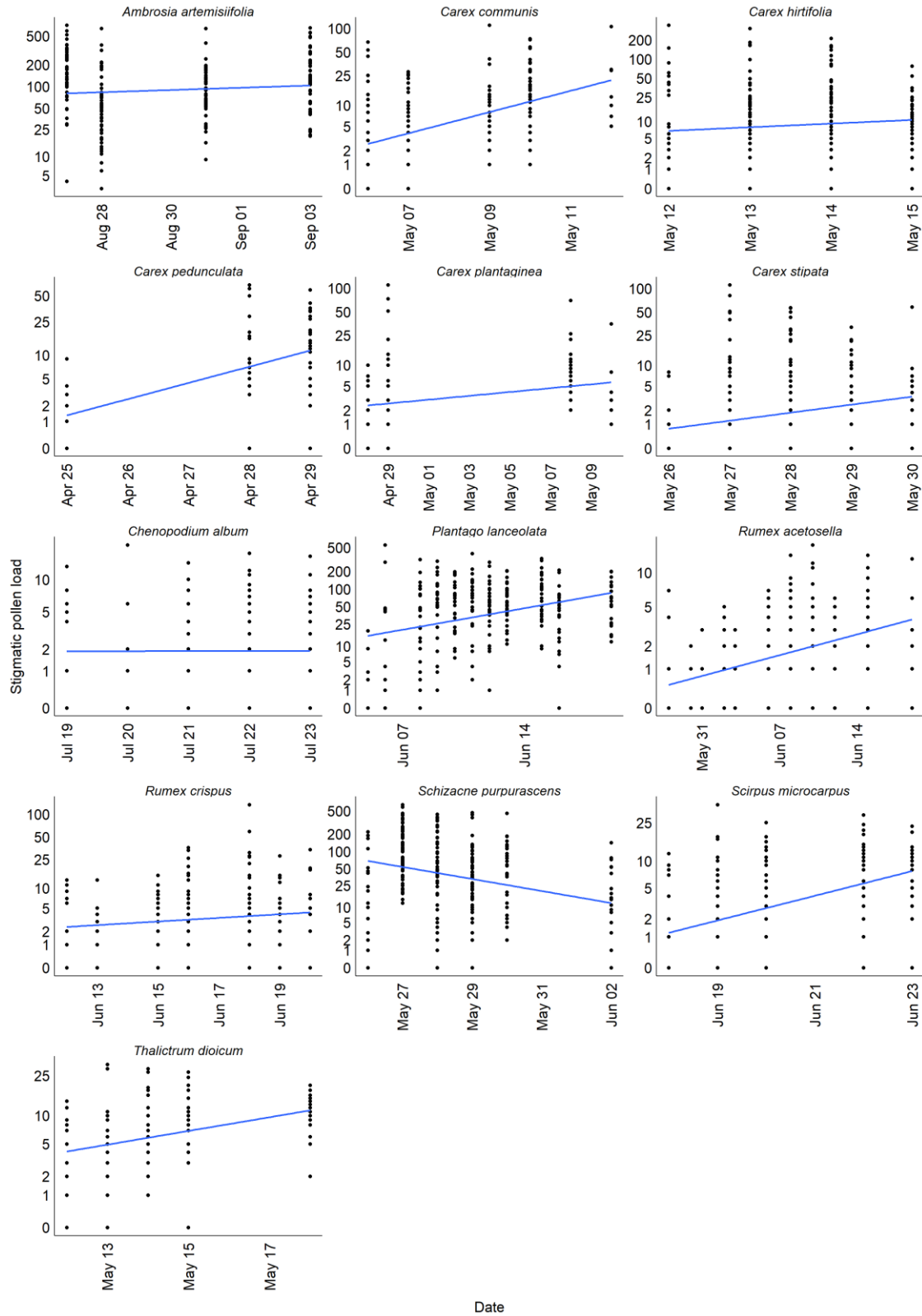


Figure B-3. Relationship between stigmatic pollen load (pollen/ovule) and sampling date. Line of best fit shown in blue.

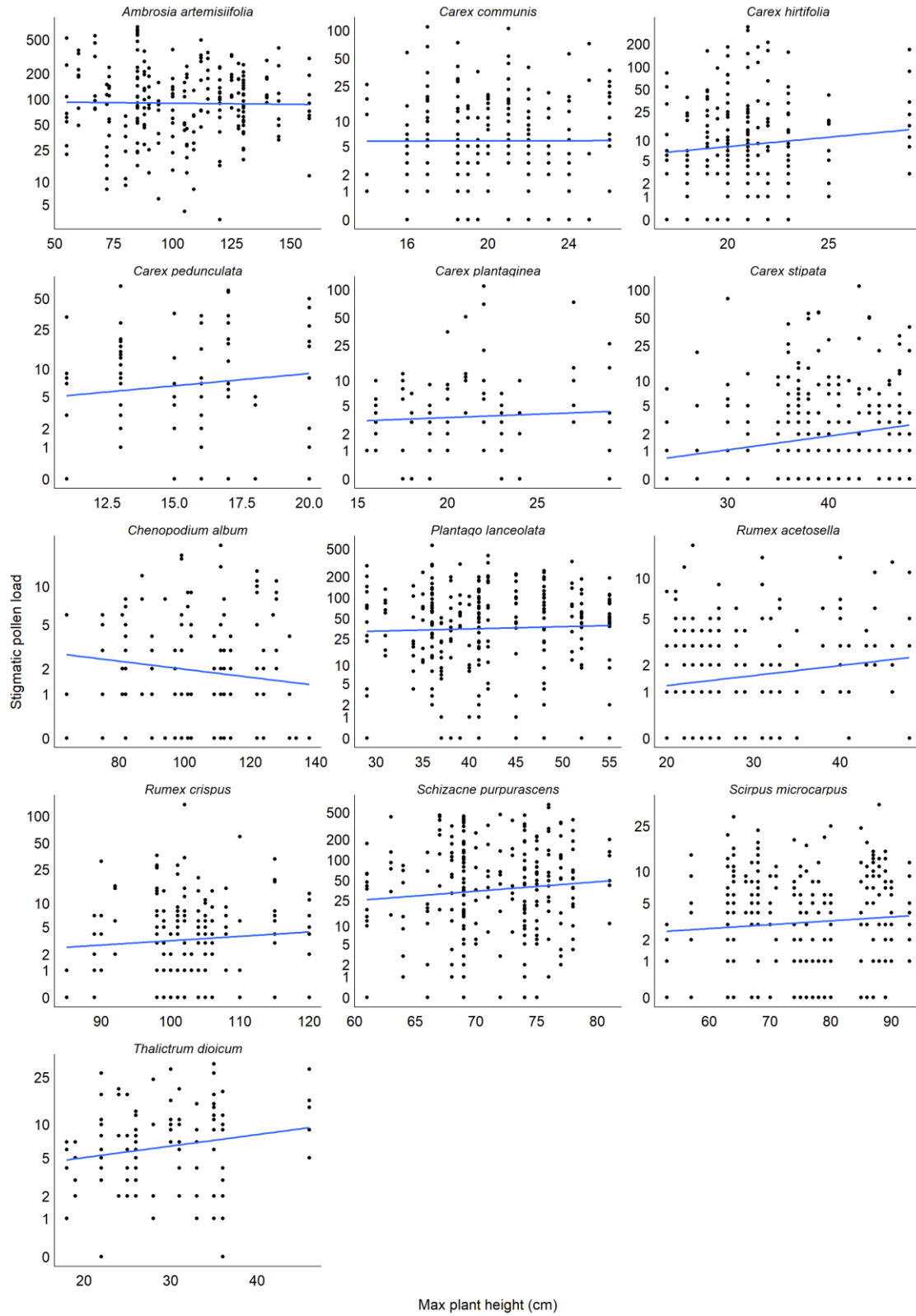


Figure B-4. Relationship between stigmatic pollen load (pollen/ovule) and plant height (cm).

Line of best fit shown in blue.

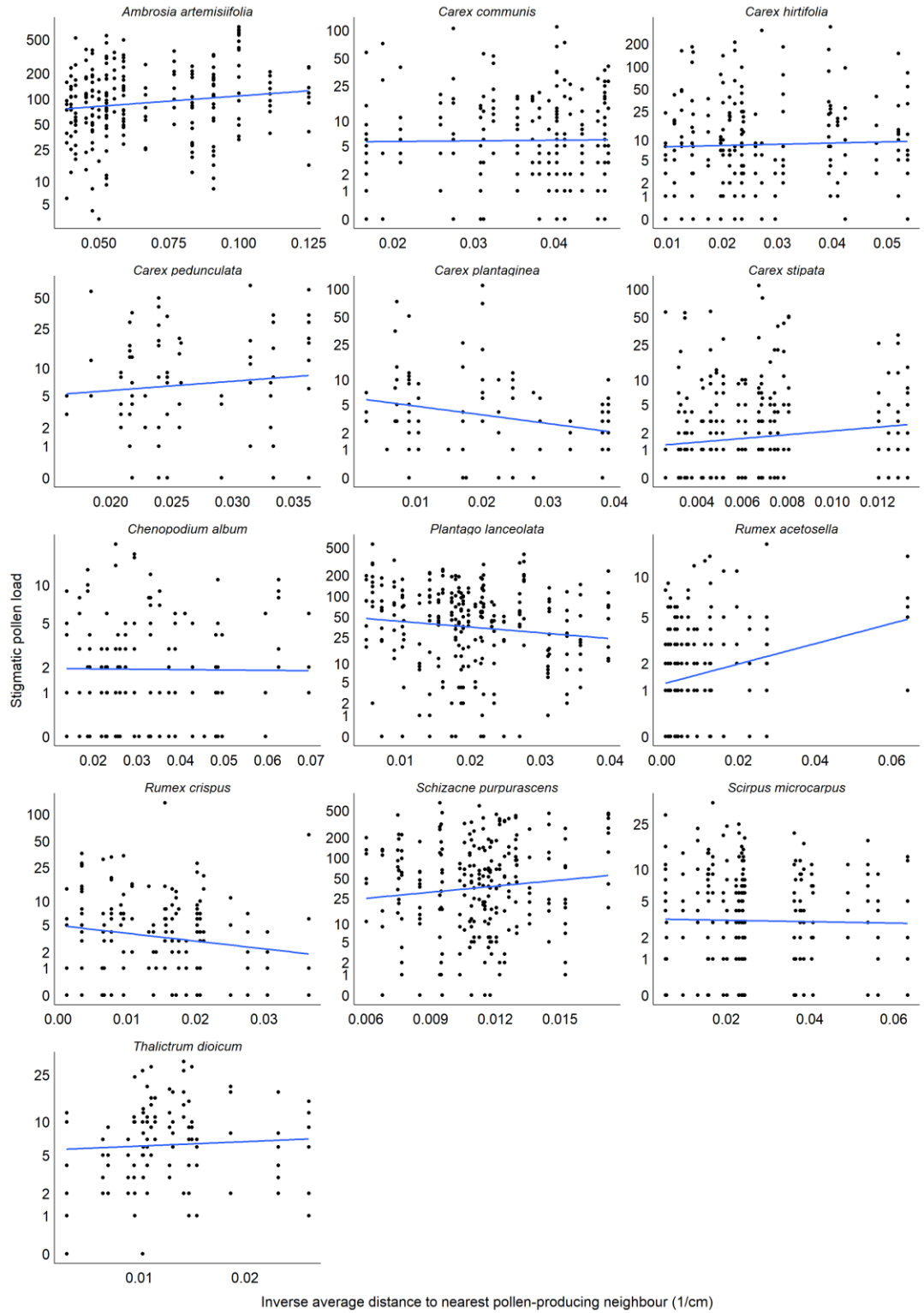


Figure B-5. Relationship between stigmatic pollen load (pollen/ovule) and density, shown as the inverse of the average distance to a plant's 5 nearest pollen-producing neighbours (cm^{-1}). Line of best fit shown in blue.

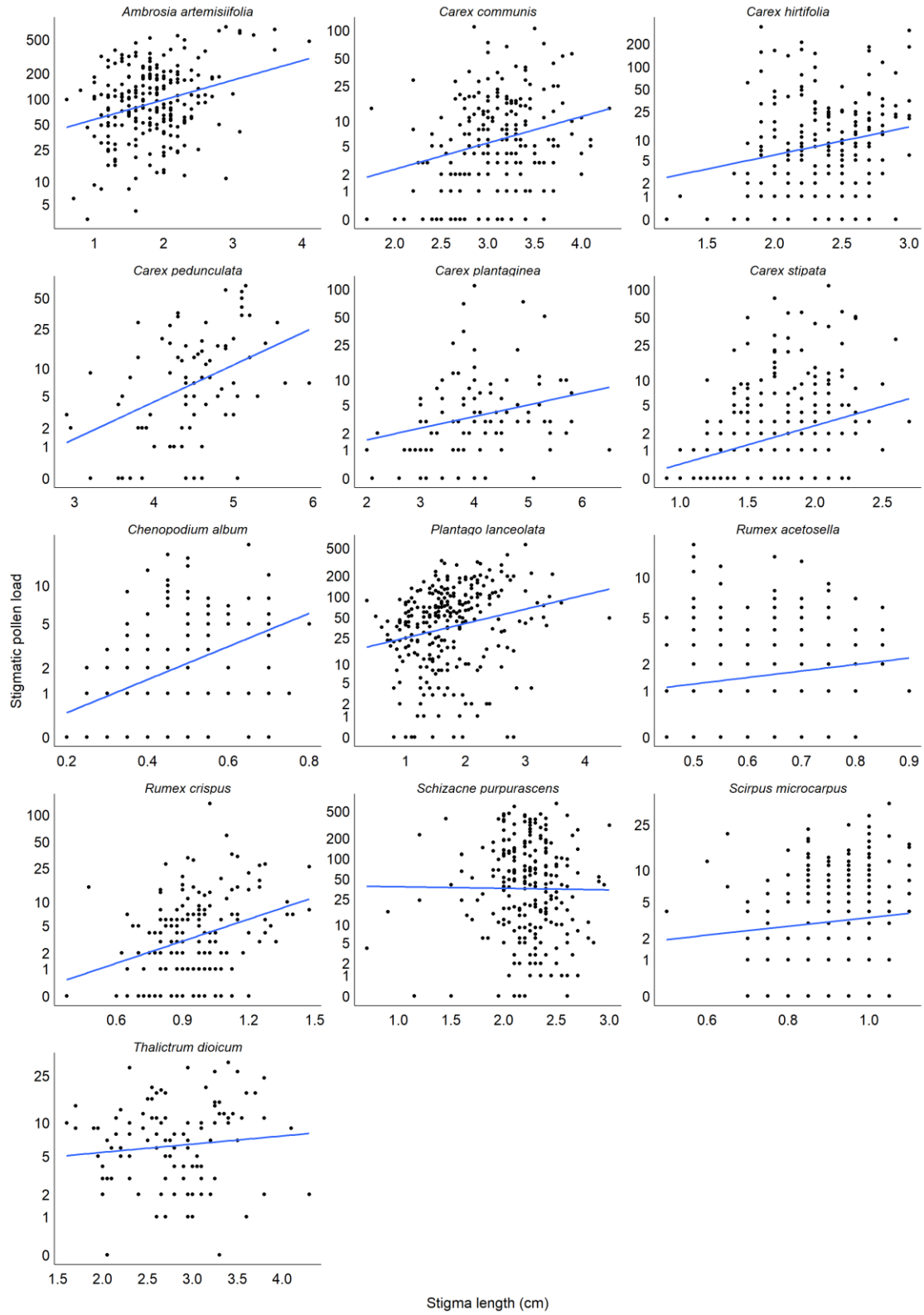


Figure B-6. Relationship between stigmatic pollen load (pollen/ovule) and stigma length (cm) for 13 wind-pollinated plants. Line of best fit shown in blue.